AD-A055 362 TEXAS UNIV AT ARLINGTON DEPT OF MECHANICAL ENGINEERING F/G 6/11
AN EVALUATION OF THE FLUIDIC OXYGEN PARTIAL PRESSURE SENSOR.(U)
DEC 77 R L WOODS F41609-76-C-0028
UNCLASSIFIED FLCS-7601 SAM-TR-77-31 NL

1 OF 1
AD A055 362

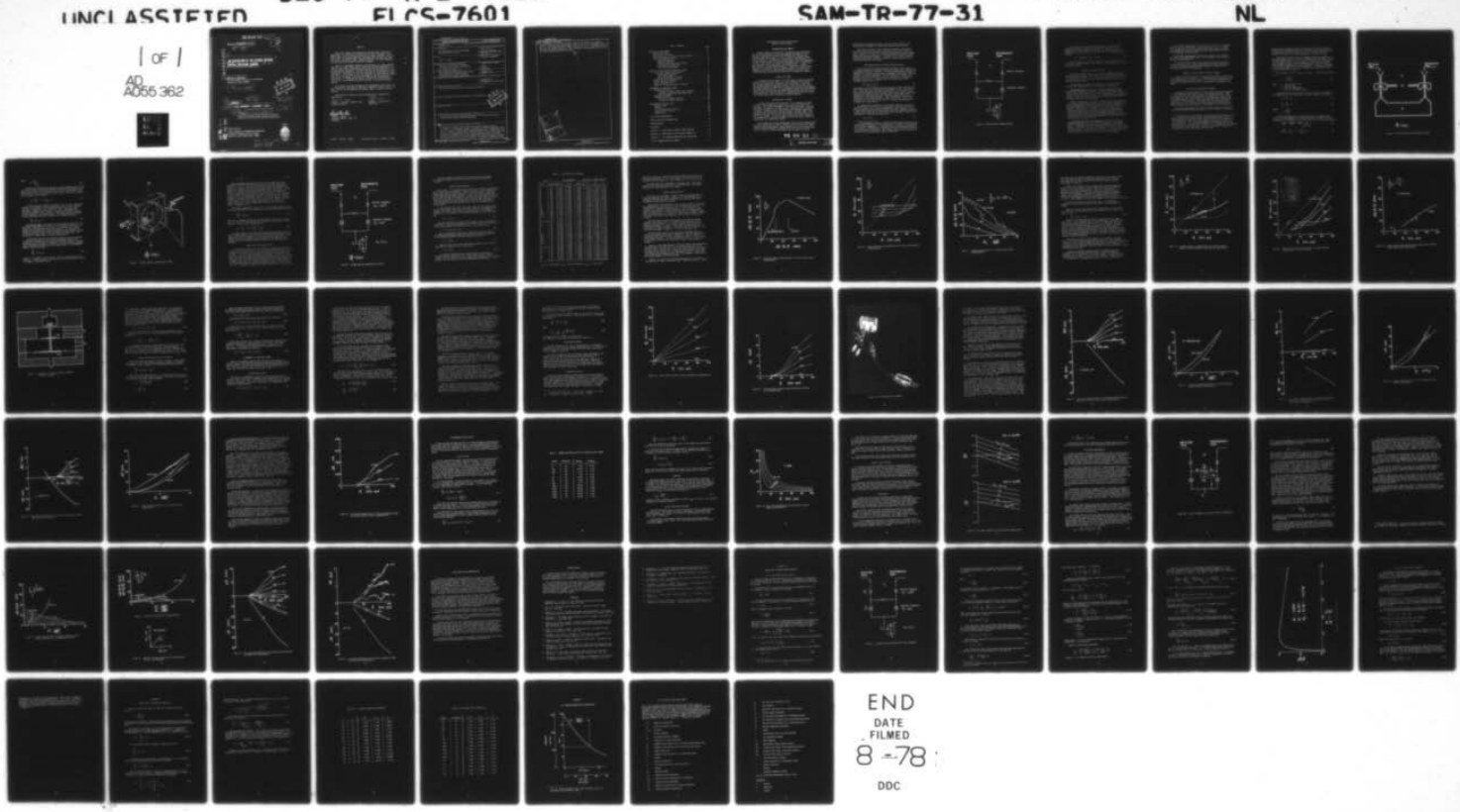

END
DATE FILMED
8-78
DDC

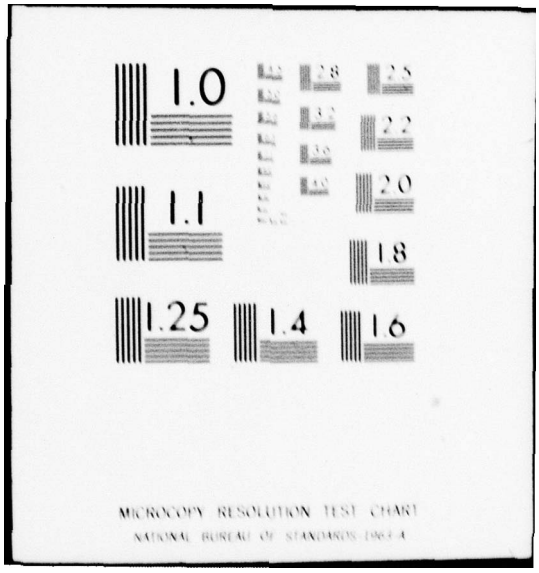
1.0
1.1
1.25
1.4
1.6
2.2
2.0
1.8
MICROCOPY RESOLUTION TEST CHART
NATIONAL BUREAU OF STANDARDS 1963-A

FOR FURTHER TRAN

Report SAM-TR-77-31

(18) (19)

(2)

AD A055362

(6) AN EVALUATION OF THE FLUIDIC OXYGEN PARTIAL PRESSURE SENSOR.

(10) Robert L. Woods
The University of Texas at Arlington
Arlington, Texas 76019

(14) FLCS-76-01

(12) 76 p.

(16) 2767

(11) Dec 77

(9) Final Report, Jan -Jul 76,

(17) 16

(15) F41609-76-C-0028

Approved for public release; distribution unlimited.

AD No.
DDC FILE COPY

Prepared for
USAF SCHOOL OF AEROSPACE MEDICINE
Aerospace Medical Division (AFSC)
Brooks Air Force Base, Texas 78235

NOTICES

This final report was submitted by the Mechanical Engineering Department, The University of Texas at Arlington, Arlington, Texas 76019, under contract F41609-76-C-0028, job order 2767164A, with the USAF School of Aerospace Medicine, Aerospace Medical Division, AFSC, Brooks Air Force Base, Texas. Captain Richard F. Stribley (SAM/VNL) was the Laboratory Project Scientist-in-Charge.

When U.S. Government drawings, specifications, or other data are used for any purpose other than a definitely related Government procurement operation, the Government thereby incurs no responsibility nor any obligation whatsoever; and the fact that the Government may have formulated, furnished, or in any way supplied the said drawings, specifications, or other data is not to be regarded by implication or otherwise, as in any manner licensing the holder or any other person or corporation, or conveying any rights or permission to manufacture, use, or sell any patented invention that may in any way be related thereto.

This report has been reviewed by the Information Office (OI) and is releasable to the National Technical Information Service (NTIS). At NTIS, it will be available to the general public, including foreign nations.

This technical report has been reviewed and is approved for publication.

Richard F. Stribley

RICHARD F. STRIBLEY, Captain, USAF
Project Scientist

R. L. Miller

RICHARD L. MILLER, Ph.D.
Supervisor

Robert G. McIver

ROBERT G. MCIVER
Brigadier General, USAF, MC
Commander

Editor: ARTHUR B. DAVIS

Supervisory Editor: MARION E. GREEN

UNCLASSIFIED

SECURITY CLASSIFICATION OF THIS PAGE (When Data Entered)

REPORT DOCUMENTATION PAGE		READ INSTRUCTIONS BEFORE COMPLETING FORM
1. REPORT NUMBER: SAM-TR-77-31	2. GOVT ACCESSION NO.	3. RECIPIENT'S CATALOG NUMBER
4. TITLE (and Subtitle): AN EVALUATION OF THE FLUIDIC OXYGEN PARTIAL PRESSURE SENSOR		5. TYPE OF REPORT & PERIOD COVERED: Final Report, Jan. 76- July 76
		6. PERFORMING ORG. REPORT NUMBER: FLCS-7601
7. AUTHOR(s): Robert L. Woods		8. CONTRACT OR GRANT NUMBER(s): F41609-76-C-0028
9. PERFORMING ORGANIZATION NAME AND ADDRESS: Mechanical Engineering Department, The University of Texas at Arlington, Arlington, TX 76019		10. PROGRAM ELEMENT, PROJECT, TASK AREA & WORK UNIT NUMBERS: 62202F, 2767164A
11. CONTROLLING OFFICE NAME AND ADDRESS: USAF School of Aerospace Medicine (VNL), Aerospace Medical Division (AFSC), Brooks Air Force Base, Texas 78235		12. REPORT DATE: December 1977
		13. NUMBER OF PAGES: 73
14. MONITORING AGENCY NAME & ADDRESS (if different from Controlling Office)		15. SECURITY CLASS. (of this report): UNCLASSIFIED
		15a. DECLASSIFICATION/DOWNGRADING SCHEDULE

16. DISTRIBUTION STATEMENT (of this Report)

Approved for public release; distribution unlimited.

17. DISTRIBUTION STATEMENT (of the abstract entered in Block 20, if different from Report)

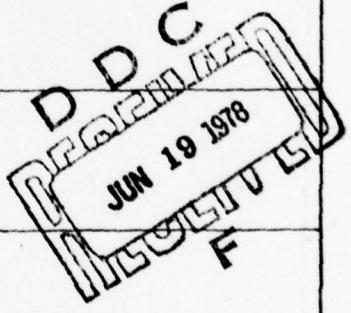

18. SUPPLEMENTARY NOTES

19. KEY WORDS (Continue on reverse side if necessary and identify by block number)

Fluidics, Sensor, Gas Concentration Sensor, Partial Pressure Sensor, Oxygen Sensor, Oxygen Breathing Regulator

20. ABSTRACT (Continue on reverse side if necessary and identify by block number)

A theoretical concept for a fluidic gas partial pressure sensor is evaluated. In the sensor concept, a fluidic resistive bridge gas concentration sensor is powered by the vacuum produced with a compressible flow ejector. Because of the ejector characteristics, the pressure drop across the bridge is proportional to the ambient pressure; hence, the sensor output is proportional to the gas concentration and the ambient pressure, the product of which is partial pressure. A complete mathematical model

DD FORM 1 JAN 73 1473 EDITION OF 1 NOV 65 IS OBSOLETE

UNCLASSIFIED

SECURITY CLASSIFICATION OF THIS PAGE (When Data Entered)

20. Abstract - continued
is derived that is in close agreement with the experiment. A prototype sensor is discussed and tested over a range of 0.3 to 1.0 atmospheres pressure and 0 to 100% concentrations of CO_2 in air and O_2 in air. The test results show that the sensor responds to both variables. Environmental sensitivities and signal amplification are discussed.

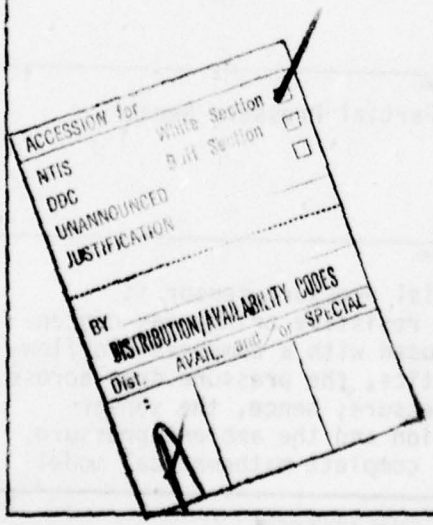

TABLE OF CONTENTS

AN EVALUATION OF THE FLUIDIC OXYGEN PARTIAL PRESSURE SENSOR

INTRODUCTION AND SUMMARY

Fluidics offers a potential for improved sensing, computation, and control requirements in military applications because of its inherent simplicity and reliability afforded by no moving parts. One major application area is in the airborne life support systems since fluidics is so compatible with the sensing requirements (e.g., suction pressure, flow rate, gas concentration, time, and temperature) as well as the control or actuation requirements (e.g., respiratory gas flow rate, gas mixture ratio, and cooling rate). In most applications, a fluid-related property is sensed and a fluid flow or pressure is controlled; thus, it appears natural to accomplish the computation, as well as the sensing and control, with the fluid itself and avoid interfaces with electrical or mechanical hardware.

Purpose and Scope

The purpose of this study is to investigate a recently developed fluidic partial pressure sensor [17] and to evaluate its potential for sensing oxygen partial pressure for application in future on-board oxygen breathing regulator systems. The scope of this report includes a theoretical description of operation, optimum design guides, environmental sensitivities, and experimental testing over the complete range of altitude pressures and oxygen concentrations expected in aircraft operations. Also included is a complete description of related fluidic gas concentration and partial pressure sensors.

Applications of Sensor

In high-altitude Air Force aircraft, it is necessary to supply the pilot with supplementary oxygen as an increasing function of altitude. This oxygen supplement is necessary to provide a sea-level equivalent of oxygen or, in other words, a constant partial pressure of oxygen. Present systems are open-loop prescheduled oxygen flow control systems based upon altitude pressure. In most cases, these regulators are not precise, and, due to their open-loop nature, are wasteful of oxygen. It would be more efficient to actually measure the oxygen partial pressure delivered to the pilot and to control the oxygen flow in a closed-loop system.

This closed-loop control necessitates the use of an oxygen partial pressure sensor that is simple, reliable, and consistent with control hardware and working medium. More importantly, a closed-loop control requires active computation meaning either electronic or fluidic circuitry. Because of these requirements and the explosion hazard

associated with electronic sensors, fluidic sensing appears to be the principal candidate for closed-loop oxygen control systems.

The sensor discussed in this report has potential applications in various forms of oxygen control systems and regulators ranging from a simple continuous control system to measure and control oxygen partial pressure in a mask, to a sophisticated phased-dilution physiological-demand oxygen regulator. In either case, a partial pressure regulator system could provide an economy of oxygen because of the closed-loop nature of the system.

Brief Description of Partial Pressure Sensor

The fluidic partial pressure sensor discussed in this report is a resistive bridge gas concentration sensor coupled with a compressible-flow ejector as shown in Figure 1. The bridge concentration sensor is composed of orifice resistors (density dependent) and laminar capillary resistors (viscosity dependent). As gas concentration varies, the density and viscosity of the mixture vary and hence, a differential pressure signal, ΔP_o, is produced that is characterized by the following equation [15, 18.].[1]

$$\Delta P_o = G_b \, S_b \, \delta P_b \, X \tag{1}$$

The term G_b is the linearized sensor gain function that expresses the basic sensor gain as a function of the geometric sizes of the resistors. While G_b varies with operating conditions, the sensor can be designed to maintain G_b nearly constant over a wide range of operation. The S_b term is the gas sensitivity constant relating the sensor's sensitivity to the gases measured. Thus, the product $G_b \, S_b$ can be considered to be a constant over a range of operation. δP_b is the pressure drop across the bridge, and X is the gas concentration of a sample gas in the mixture.

A compressible flow ejector (or jet pump) produces a vacuum that is used to entrain the mixture and reference gases into the sensor. When the ejector with a pressure-scheduled pressure regulator is used to power the bridge, the bridge pressure drop, δP_b, becomes proportional to the ambient pressure, P_a, which varies with altitude. (Again, this expression is linearized and idealized.)

$$\delta P_b = C_1 \, P_a \tag{2}$$

---

[1] The mathematical analysis involves nonlinear equations that can be linearized as discussed in the references and in detail in the remainder of this report (Appendix A). The description of operation presented in this section is linearized and idealized for the sole purpose of explaining the concepts of operation. The nonideal effects are considered and specified for design purposes later in the report.

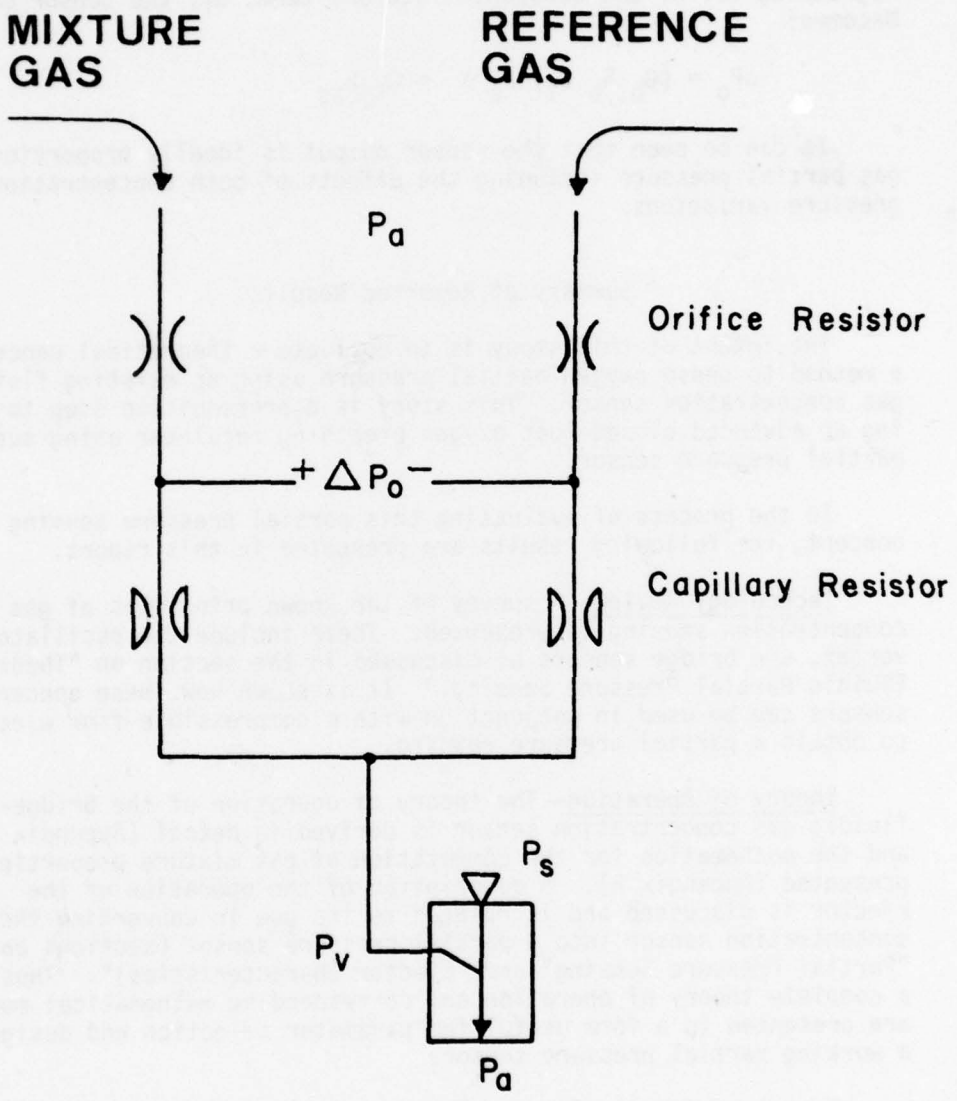

Figure 1. Fluidic partial pressure sensor.

This variation in bridge pressure drop has a multiplicative effect with the gas concentration so that the output signal is proportional to the gas partial pressure, $P_{\partial s}$ (since $P_{\partial s} = P_a X$). Regrouping all of the constants into one term, G_T, the sensor output becomes:

$$\Delta P_o = (G_b S_b C_1) P_a X = G_T P_{\partial s} \quad (3)$$

It can be seen that the sensor output is ideally proportional to gas partial pressure including the effects of both concentration and pressure variations.

Summary of Reported Results

The intent of this study is to evaluate a theoretical concept of a method to sense oxygen partial pressure using an existing fluidic gas concentration sensor. This study is a prerequisite step to building an advanced closed-loop oxygen breathing regulator using such a partial pressure sensor.

In the process of evaluating this partial pressure sensing concept, the following results are presented in this report.

Technology Review--A survey of the known principles of gas concentration sensing is presented. These include the oscillator, vortex, and bridge sensors as discussed in the section on "Theory of Fluidic Partial Pressure Sensing." It is shown how these concentration sensors can be used in conjunction with a compressible-flow ejector to obtain a partial pressure reading.

Theory of Operation--The theory of operation of the bridge-type fluidic gas concentration sensor is derived in detail (Appendix A) and the mathematics for the computation of gas mixture properties is presented (Appendix B). A description of the operation of the ejector is discussed and is related to its use in converting the concentration sensor into a partial pressure sensor (sections on "Partial Pressure Sensing" and "Ejector Characteristics)". Thus a complete theory of operation and corresponding mathematical model are presented in a form useful for parameter selection and design of a working partial pressure sensor.

Prototype Fabrication and Testing--A discussion of sizing, parameter selection, and other trade-offs required in the system design is presented in the section on "Performance of Prototype Sensor." Prototype sensors were fabricated using parts from existing Air Force sensors [6] and discrete components. These modified sensors were tested over a complete map of concentrations (varying from 0 to 100% O_2) and pressures (ranging from 0.3 to 1.0 atmosphere).

Environmental Sensitivity--The sensitivity of the partial pressure sensor to various environmental or uncontrollable effects is studied. This includes the sensitivity to other gases which might be present including humidity, ambient temperature, and supply pressure (section on "Environmental Sensitivities").

Utilization Requirements--Contamination filtering, gas chemical processing, and signal amplification are considered in the section on "Utilization Requirements."

It is shown from the theory and experimental results presented in this report that the fluidic oxygen partial pressure sensor can be utilized in advanced oxygen breathing regulators to improve their performance by closed-loop operation.

THEORY OF FLUIDIC PARTIAL PRESSURE SENSING

In this section three types of concentration sensors are identified and mathematically described. It is shown how each concentration sensor can be made to sense partial pressure. This review is presented for reference information and only one of the sensors is evaluated in this report.

Fluidic Gas Concentration Sensors

Currently three known types of fluidic sensors have been discussed in the literature: oscillator, vortex, and resistive bridge. There are naturally variations upon these basic principles that will not be discussed here. Each sensor discussed is provided with a mixture and a reference channel so that relative concentration rather than absolute properties will be measured. The sensors discussed are powered by a vacuum source so that the gases to be measured can be entrained from ambient pressure and would not have to be pumped to positive pressure.[2]

Oscillator-Type Sensor--The oscillator-type sensor was identified at the Harry Diamond Laboratories (HDL) in the early days of fluidics as

[2]In the discussion that follows, the following nomenclature will be used to identify the various gases: The term "mixture gas" refers to a combination of a "sample gas" whose concentration in a "reference gas" is to be measured. This study uses oxygen as the sample gas and air as the reference gas. The mixture concentration of the sample gas in the reference gas, X_S, can vary from 0 to 100%. It is assumed that the unknown concentration of the sample gas is the only difference in the gases in the mixture and reference channels of the sensor.

being a device of great utility. The primary use of the oscillating sensor was for temperature sensing. Later this type of sensor was used to sense concentrations of CO_2 and O_2 in air for respiratory gas analysis [14], and for related concentration sensing [3, 8, 12].

This sensor utilizes a sonic or feedback oscillating amplifier in which the frequency of oscillation is dependent upon the speed of sound and the feedback length. As a fraction of a sample gas is introduced into the reference gas, the gas properties, and hence the acoustic speed, change in proportion to the concentration. Thus, the frequency of oscillation changes with gas concentration. A reference oscillator is usually provided so that a beat frequency can be monitored. This system is depicted in Figure 2.

The frequency, f, of a fluidic oscillator is given by the following [1, 7]:

$$f = \frac{\sqrt{k\, R_r\, T_a}}{2L} \tag{4}$$

where k = specific heat ratio,
R_r = gas constant,
T_a = absolute temperature,
L = cavity or feedback length

Using two oscillators, one for the mixture gas (m) and another for the reference gas (r), the difference or beat frequency is given by:

$$\Delta f = f_m - f_r \tag{5}$$

$$\frac{\Delta f}{f_r} = \frac{L_r}{L_m}\sqrt{U} - 1 \tag{6}$$

where:

$$U = \frac{k_m R_m}{k_r R_r} \tag{7}$$

The gas properties of the mixture vary with the concentration ratio, X, of the sample gas in the reference gas. Equation 6 can be expanded in a first-order Taylor series about X=0 to yield the following:

$$\frac{\Delta f(X)}{f_r} = \frac{\Delta f(X=0)}{f_r} + \frac{\partial \Delta f/fr}{\partial U}\bigg|_{U=1} \frac{\partial U}{\partial X}\bigg|_{X=0} X_s \tag{8}$$

$$\frac{\Delta f(x)}{f_r} = \left(\frac{L_r}{L_m} - 1\right) + \left(\frac{1}{2}\frac{L_r}{L_m}\right) S_o\, X_s \tag{9}$$

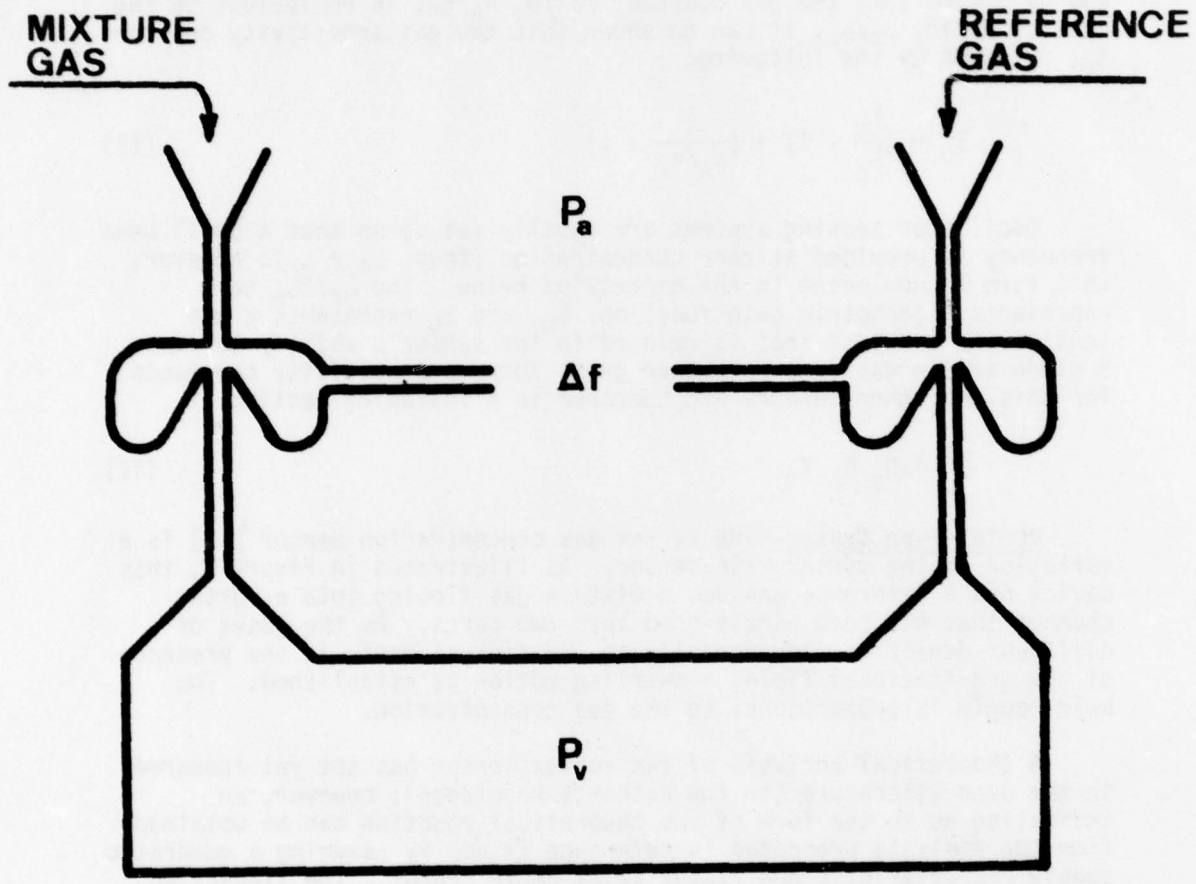

$$\frac{\Delta f}{f} = G_o S_o X_s$$

Figure 2. Oscillator-type gas concentration sensor.

where:

$$S_o = \left.\frac{\partial U}{\partial X}\right|_{X=0} \tag{10}$$

Assuming that the specific heat ratio and gas constant for a mixture (m) can be linearly interpolated between the reference and sample values, and by noting that the gas constant ratio, R_s/R_r, is equivalent to the density ratio, ρ_r/ρ_s, it can be shown that the gas sensitivity constant, S_o, is given by the following:

$$S_o = \left(\frac{k_s}{k_r} - 1\right) + \left(\frac{1}{\rho_s/\rho_r} - 1\right) \tag{11}$$

Oscillator sensing systems are usually set up so that a small beat frequency is provided at zero concentration (thus, $L_m \neq L_r$); however, this term is neglected in the expression below. The $L_r/2L_m$ term represents a geometric gain function, G_o, and S_o represents a gas sensitivity constant that is related to the sensor's ability to sense a given sample gas in a reference gas. The gas sensitivity constants for this and other sensors are compared in a following section.

$$\frac{\Delta f}{f_r} = G_o\, S_o\, X_s \tag{12}$$

Vortex-Type Sensor--The vortex gas concentration sensor [11] is a variation of the vortex rate sensor. As illustrated in Figure 3, this device has a reference gas and a mixture gas flowing into a vortex chamber that has been partitioned into two parts. As the gases of different densities flow radially to the central drain in the presence of the gravitational field, a swirling motion is established. The swirl angle is proportional to the gas concentration.

A theoretical analysis of the vortex sensor has not yet appeared in the open literature (to the author's knowledge); however, an indication as to the form of the theoretical equation can be obtained from the analysis presented in reference 11 and by assuming a quadratic supply characteristic and linear swirl angle sensor. The linearized result is given as follows:

$$\frac{\Delta P_o}{\delta P_b} = G_v\, S_v\, X_s \tag{13}$$

where G_v is a geometric gain function, and S_v is the gas sensitivity constant. From the analysis, the vortex sensor gas sensitivity constant is related to the density ratio.

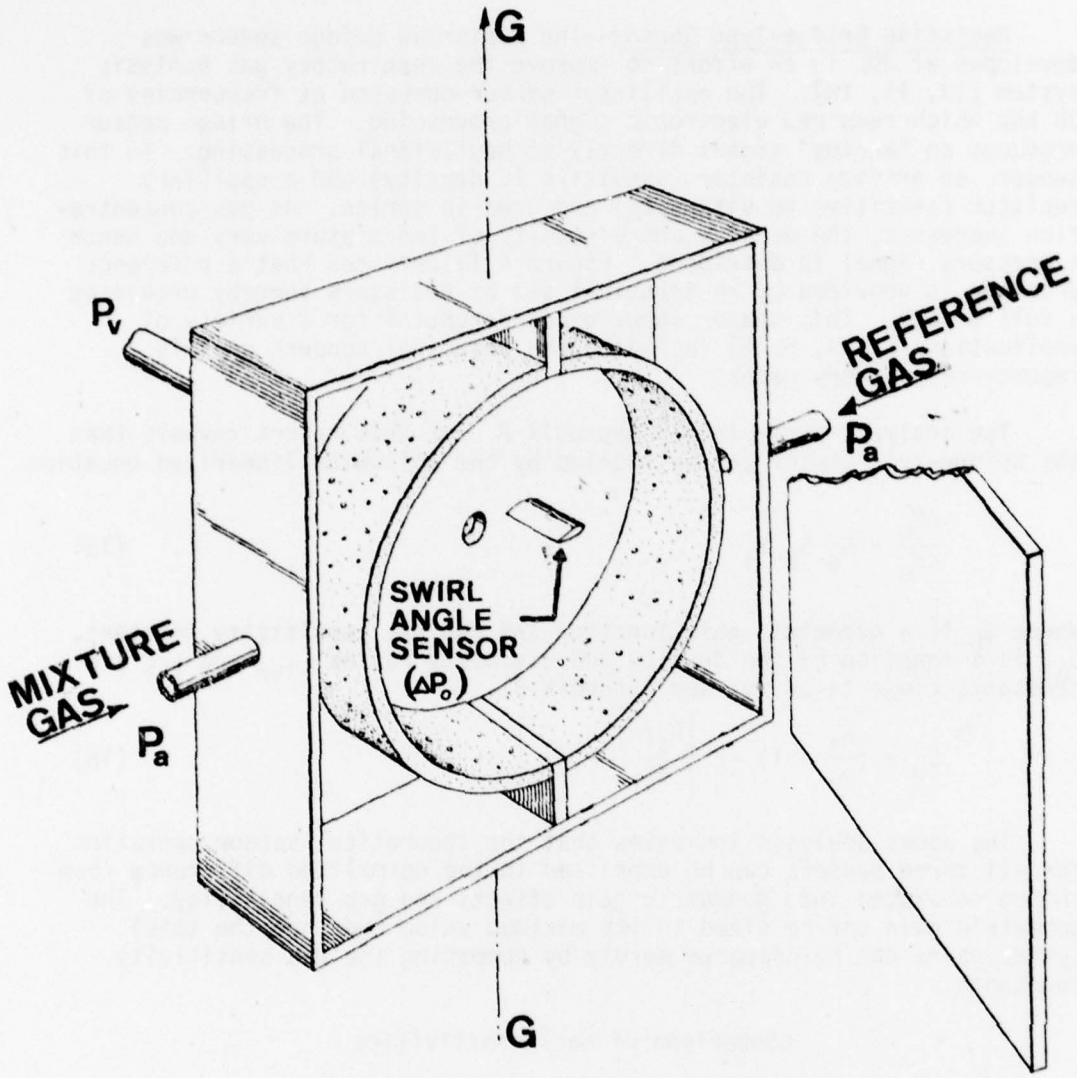

$$\frac{\Delta P_o}{\delta P_b} = G_v S_v X_s$$

Figure 3. Vortex-type gas concentration sensor.

$$S_v = \left(\frac{\rho_s}{\rho_r} - 1\right) \tag{14}$$

Resistive Bridge-Type Sensor--The resistive bridge sensor was developed at HDL in an effort to improve the respiratory gas analysis system [13, 15, 18]. The oscillator sensor operated at frequencies of 30 kHz which required electronic signal processing. The bridge sensor produces an "analog" signal directly without signal processing. In this sensor, an orifice resistor (sensitive to density) and a capillary resistor (sensitive to viscosity) are used in series. As gas concentration increases, the density and viscosity of the mixture vary and hence a pressure signal is developed. Figure 4 illustrates that a reference pressure is provided by an identical set of resistors thereby providing a full bridge. This sensor shows great potential for a variety of applications [2, 4, 5, 6] including the principal concern of this report--respiratory gases.

The analysis presented in Appendix A of this report reveals that the bridge-type sensor can be modeled by the following linearized equation.

$$\frac{\Delta P_o}{\delta P_b} = G_b \, S_b \, X_s \tag{15}$$

Where G_b is a geometric gain function and the gas sensitivity constant, S_b, is a function of the density and viscosity ratios (ϕ_{sr} and ϕ_{rs} are constants close to unity; see Appendix B).

$$S_b = \left(\frac{\rho_s}{\rho_r} - 1\right) - 2 \left| \frac{\mu_s/\mu_r}{\phi_{sr}} - \phi_{rs} \right| \tag{16}$$

The above analysis indicates that the theoretical sensor operation for all three sensors can be expressed in the normalized difference form and be separated into geometric gain effects and gas sensitivity. The geometric gain can be sized to its maximum value and then the total system gains can be compared merely by comparing the gas sensitivity constants.

Comparison of Gas Sensitivities

To compare the sensors for their ability to properly measure the concentration of any given gas, it is desirable that the gas sensitivity constant for the given gas be large and the sensitivity to other gases be small. This will insure that even if other gases are present, the sensor will not significantly measure their effect. If this is not the case, care should be taken that the concentration level of spurious gases present be low. This may require chemical processing of the sample gas to remove other gases (e.g., dryers, absorbers, etc.). A gas mixture is the reference gas plus an unknown concentration ratio, X, of the sample gas. It is assumed that there are no other differences in the two gases.

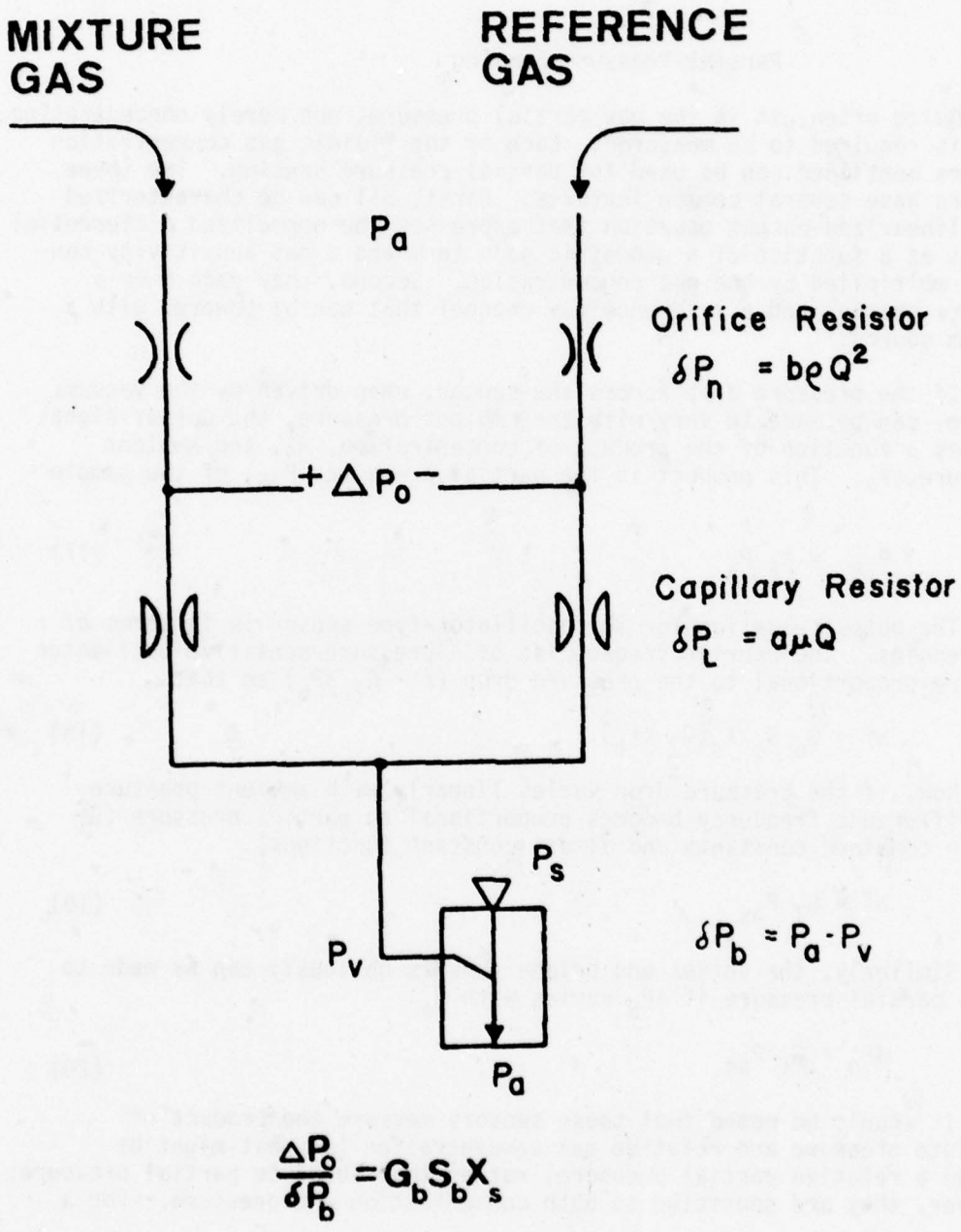

Figure 4. Bridge-type gas concentration sensor.

The single-sample gas sensitivities of the three basic sensors for a variety of gases in different reference gases are summarized in Table 1.

Partial Pressure Sensing

Quite often, it is the gas partial pressure, not merely concentration, that is required to be measured. Each of the fluidic gas concentration sensors mentioned can be used for partial pressure sensing. The three sensors have several common features. First, all can be characterized by a linearized output equation that expresses the normalized differential output as a function of a geometric gain term and a gas sensitivity constant multiplied by the gas concentration. Second, they each have a mixture channel and a reference gas channel that can be powered with a vacuum source.

If the pressure drop across the sensor, when driven by the vacuum source, can be made to vary with the ambient pressure, the output signal becomes a function of the product of concentration, X_s, and ambient pressure, P_a. This product is the partial pressure, $P_{\partial s}$, of the sample gas.

$$P_{\partial s} = X_s P_a \tag{17}$$

The output equation for the oscillator-type sensor is in terms of frequencies. The carrier frequencies of a pressure-sensitive oscillator [1] are proportional to the pressure drop ($f = C_2 \delta P_b$) so that

$$\Delta f = G_o S_o X_s (C_2 \delta P_b) \tag{18}$$

Now, if the pressure drop varies linearly with ambient pressure, the difference frequency becomes proportional to partial pressure (G_T is the combined constants and almost constant functions).

$$\Delta f = G_T P_{\partial s} \tag{19}$$

Similarly, the vortex and bridge sensors obviously can be made to sense partial pressure if δP_b varies with P_a.

$$\Delta P_o = G_T P_{\partial s} \tag{20}$$

It should be noted that these sensors measure the product of absolute pressure and relative gas concentration (or what might be termed a relative partial pressure) rather than absolute partial pressure; however, they are sensitive to both concentration and pressure. For a

TABLE 1. GAS SENSITIVITY CONSTANTS

CASES		GAS PROPERTIES			OSCILLATOR	VORTEX	BRIDGE
Sample	Reference	ρ_s/ρ_r	μ_s/μ_r	k_s/k_r	S_o	S_v	S_b
CO_2	Air	1.529	0.809	0.929	-0.417	0.529	1.056
O_2	Air	1.105	1.104	0.999	-0.097	0.105	-0.105
H_2O	Air	0.622	0.402	0.948	0.557	-0.378	0.764
CO	Air	0.967	0.956	1.001	0.035	-0.033	0.055
N_2	Air	0.967	0.956	1.001	0.035	-0.033	0.055
N_2O	Air	1.530	0.803	0.929	-0.413	0.523	1.075
NO	Air	1.037	1.025	0.998	-0.037	0.037	-0.014
H_2	Air	0.070	0.478	1.005	13.394	-0.934	-0.891
H_2S	Air	1.190	0.683	0.941	-0.219	0.190	1.080
He	Air	0.138	1.061	1.183	6.424	-0.862	-1.123
SO_2	Air	2.264	0.683	0.920	-0.639	1.264	2.406
CH_4	Air	0.554	0.594	0.034	0.738	-0.446	0.283
C_2H_6	Air	1.049	0.492	0.870	-0.177	0.049	1.677
C_3H_8	Air	1.554	0.437	0.805	-0.551	0.554	2.983
C_4H_{10}	Air	2.086	0.399	0.741	-0.779	1.086	4.281
C_5H_{12}	Air	2.615	0.363	0.677	-0.940	1.615	5.631
C_8H_{18}	Air	4.151	0.289	0.442	-1.317	3.150	9.658
A	Air	1.357	1.235	1.190	-0.072	0.357	-0.162
Ne	Air	0.685	1.727	1.169	0.629	-0.315	-1.146
Halothane	Air	7.315	0.765	0.500	-1.363	6.315	6.499
CO_2	O_2	1.383	0.733	0.931	-0.346	0.383	1.153
H_2O	O_2	0.562	0.446	0.949	0.728	-0.438	0.797
N_2O	O_2	1.384	0.728	0.930	-0.348	0.384	1.172
He	O_2	0.125	0.961	1.185	7.191	-0.875	-1.089
A	O_2	1.227	1.119	1.192	0.007	0.277	-0.033
Ne	O_2	0.620	1.564	1.171	-0.785	-0.381	-1.042
CH_4	O_2	0.502	0.538	0.935	0.929	-0.498	0.321
C_2H_6	O_2	0.949	0.446	0.871	-0.076	-0.051	1.726
C_3H_8	O_2	1.406	0.496	0.807	-0.482	0.406	3.041
C_4H_{10}	O_2	1.887	0.361	0.785	-0.685	0.887	4.343
C_5H_{12}	O_2	2.366	0.329	0.717	-0.860	1.366	5.694
C_8H_{18}	O_2	3.755	0.262	0.715	-1.019	2.755	9.710
Air	O_2	0.905	0.906	1.001	0.107	-0.095	0.091
N_2	O_2	0.875	0.866	1.002	0.145	-0.125	0.141
Halothane	O_2	6.618	0.693	0.360	-1.489	5.618	6.573
O_2	He	8.007	1.041	0.844	-1.031	7.007	4.839
CO_2	He	11.076	0.763	0.786	-1.124	10.076	9.683
H_2O	He	4.505	0.464	0.801	-0.977	3.505	6.952
O_2	N_2	1.143	2.254	0.998	-0.127	0.143	-0.168
CO_2	N_2	1.581	0.846	0.929	-0.439	0.581	0.987
H_2O	N_2	0.643	0.514	0.947	0.504	-0.357	0.729
H_2	N_2	0.072	0.501	1.004	12.932	-0.928	-0.903

ρ_{air} = 1.2046 kg/m^3 , μ_{air} = 183.10^{-6} gm/cm sec, γ_{air} = 1.403 at STP

true partial pressure reading, the reference channel must be free of any of the sample gas, or an initial output offset must be provided to account for the sample gas in the reference (e.g., 21% O_2 in air).

The above review is presented for reference only. The bridge sensor is the only sensor evaluated in this study and is considered exclusively in the remainder of this report.

Ejector Characteristics

An ejector, or jet pump, is used to develop the vacuum used to power the concentration sensor; however, it is the characteristic of a compressible flow ejector that permits the multiplicative effect required to measure partial pressure.

Compressible flow ejectors have two distinct regimes of operation: the incompressible and the choked. The incompressible regime can be analyzed using incompressible equations. In this operation, the pressure gain (amount of vacuum produced divided by supply pressure drop) is constant and is a function of the area ratio between vacuum port and supply nozzle flow areas [9]. Thus vacuum increases linearly with supply pressure drop as shown by the left part of the curve in Figure 5.

Once the ejector becomes fully choked, the absolute pressure created at the vacuum port, P_V, becomes a linear function of the absolute supply pressure, P_S. In this regime, further decreases in downstream pressure, P_a, have no effect upon the pressure at the vacuum port as shown in Figure 6. Notice further from Figure 6, that once the flow becomes choked, P_V is a linear function of P_S.

The preliminary tests of this study were conducted using the venturi-type ejector described in reference 6. Several modifications in geometry were tried including supersonic designs in an effort to obtain lower pressures. It was concluded that there is a fixed limit on the amount of vacuum the single-nozzle venturi-type ejector can achieve.

Figures 5 and 6 show data with infinite external load impedance at the vacuum port, and hence reflect the maximum vacuum that can be created. When an actual load, such as the sensor bridge, is placed at the vacuum port, the pressure is reduced by the product of the output resistance of the ejector, R_O, and the vacuum flow, Q_V. Thus in the actual application, loading effects must be considered in determining the vacuum produced to drive the sensor.

Figure 7 is a plot of the output characteristic of an ejector illustrating its output resistance effect. When the ejector is loaded

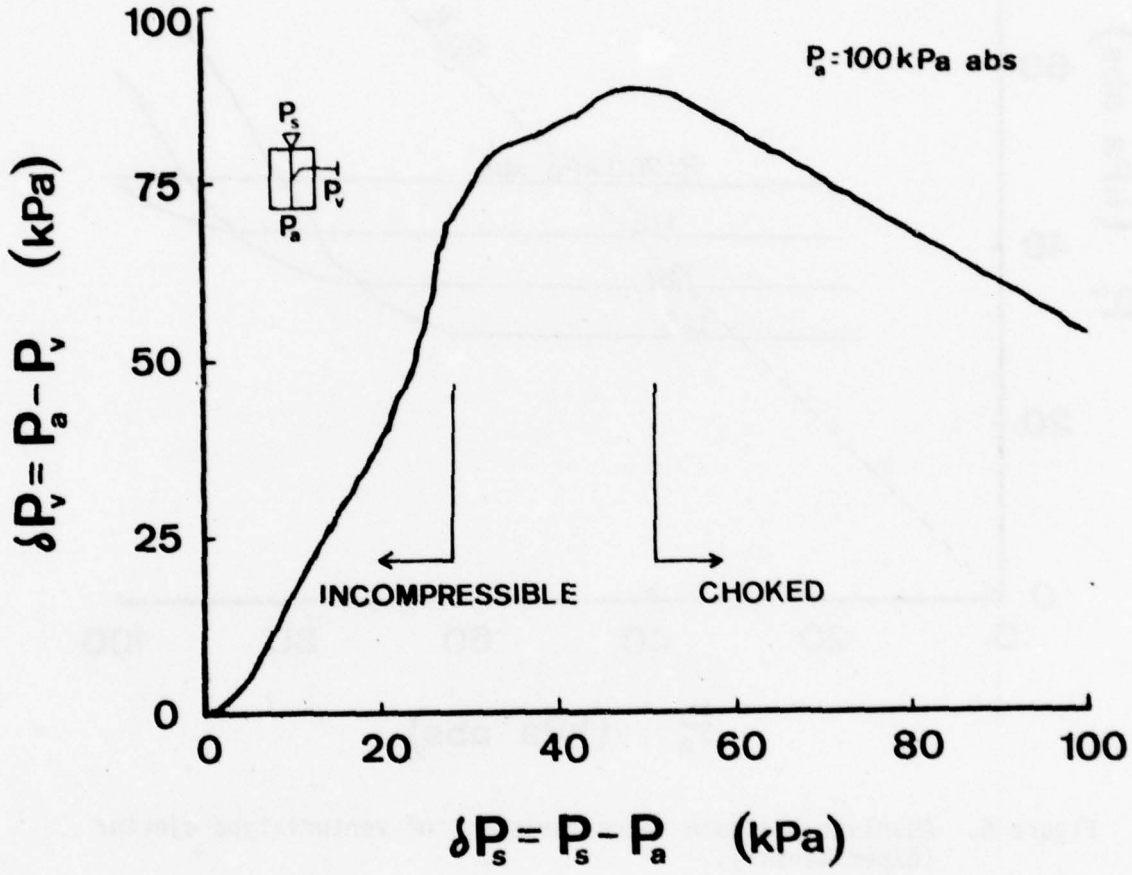

Figure 5. Pressure transfer characteristic of venturi-type ejector (experimental).

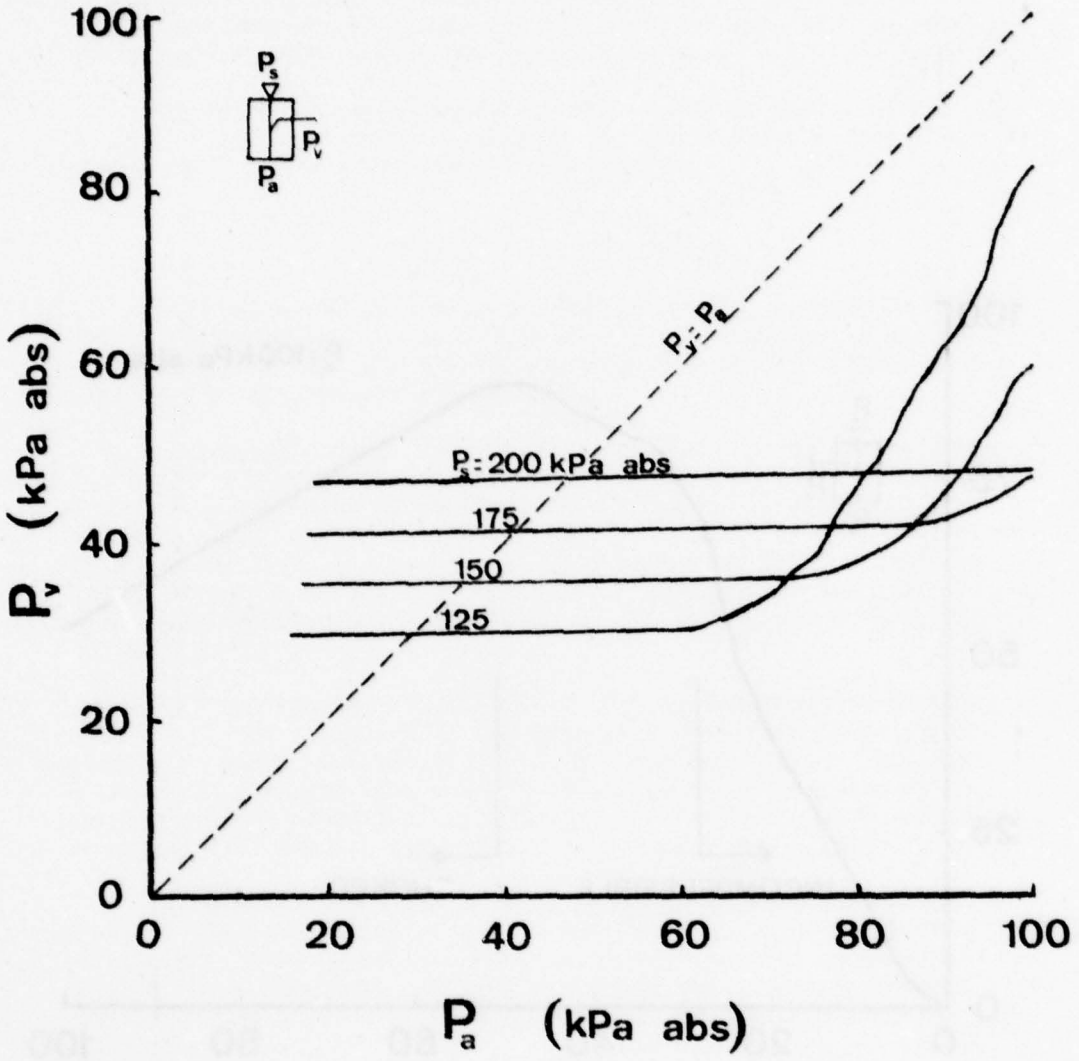

Figure 6. Absolute pressure characteristics of venturi-type ejector (experimental).

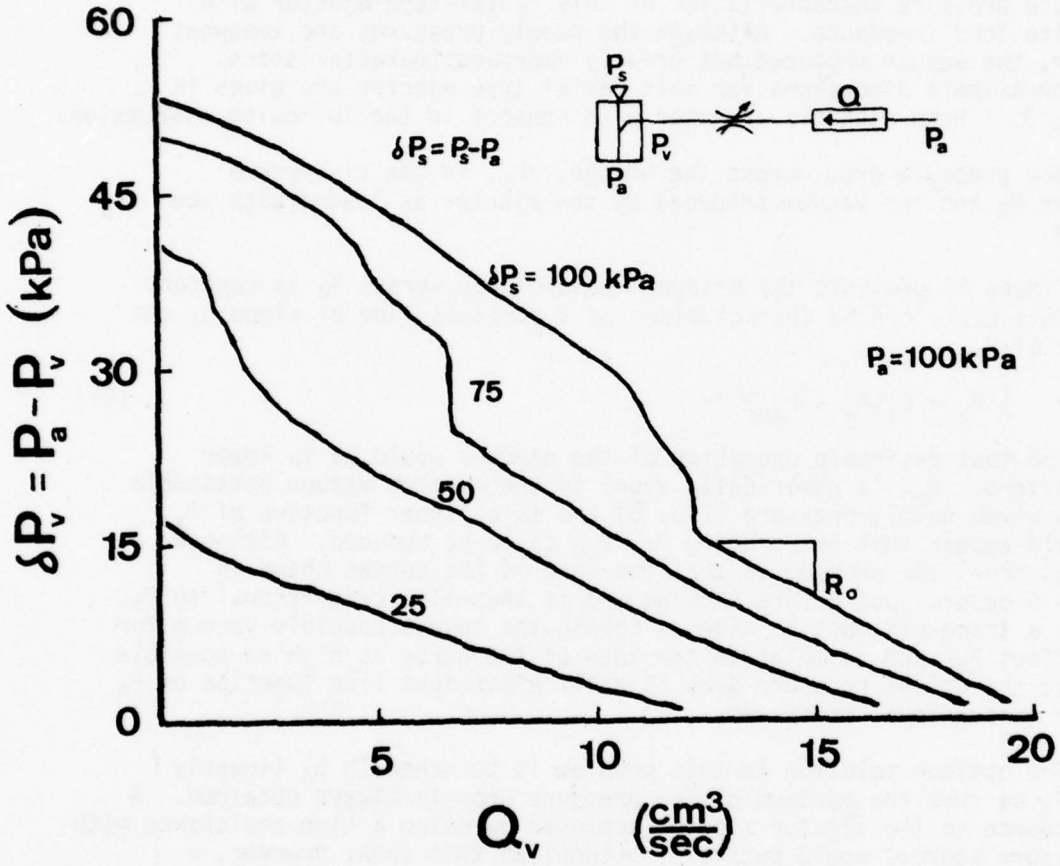

Figure 7. Output characteristic of a venturi-type ejector (experimental).

with the bridge, the absolute pressure characteristics no longer remain flat, but rather become an intermediate curve between the infinite load characteristic (dotted line) and the ambient pressure (dashed line) shown in Figure 8.

A radial flow diffuser ejector, commercially available under the name of "Mini-Vac," produces a high vacuum level and has performance similar to the venturi-type ejector. Figure 9 illustrates the absolute pressure characteristics of this radial-type ejector with infinite load impedance. Although the supply pressures are somewhat higher, the vacuum produced has greatly improved characteristics. The approximate dimensions for this radial-type ejector are given in Figure 9. Both ejectors are used with sensors in the following discussion.

The pressure drop across the bridge, δP_b, is the difference between P_a and the vacuum produced by the ejector as loaded with the sensor.

Figure 10 presents the bridge pressure drop versus P_a at constant P_s. This curve can be characterized by a straight line of slope C_1 and offset of P_{ao}.

$$\delta P_b = C_1(P_a - P_{ao}) \tag{21}$$

The most desirable operation of the ejector would be to lower P_{ao} to zero. P_{ao} is numerically equal to the maximum vacuum obtainable with a given supply pressure (Fig. 6) and is a linear function of P_s. It would appear that by reducing P_s, P_{ao} could be reduced. Although this is true, the problem is that the knee of the curves shown in Figure 6 occurs just before choking and is thus also proportional to P_s. Hence, a trade-off must be made to obtain the lowest possible vacuum for the offset P_{ao} and to maintain the knee of the curve as high as possible so that the bridge pressure drop is still a straight line function of P_a closer to sea level pressures.

The optimum solution to this problem is to schedule P_s linearly with P_a so that the maximum bridge pressure drop is always obtained. A flow source to the ejector supply (achieved by using a high resistance with a pressure source) would partially accomplish this task; however, a scheduled pressure regulator (requiring moving parts) using aneroids appears to be the best solution.

A pressure scheduled pressure regulator has been built and evaluated for the purpose discussed above. Although a scheduled regulator can be constructed in a variety of ways, a method using two diaphragms was selected. A sketch of the regulator is shown in Figure 11. In operation, an unregulated pressure, Pu, (Pu > 200 kPa abs.)

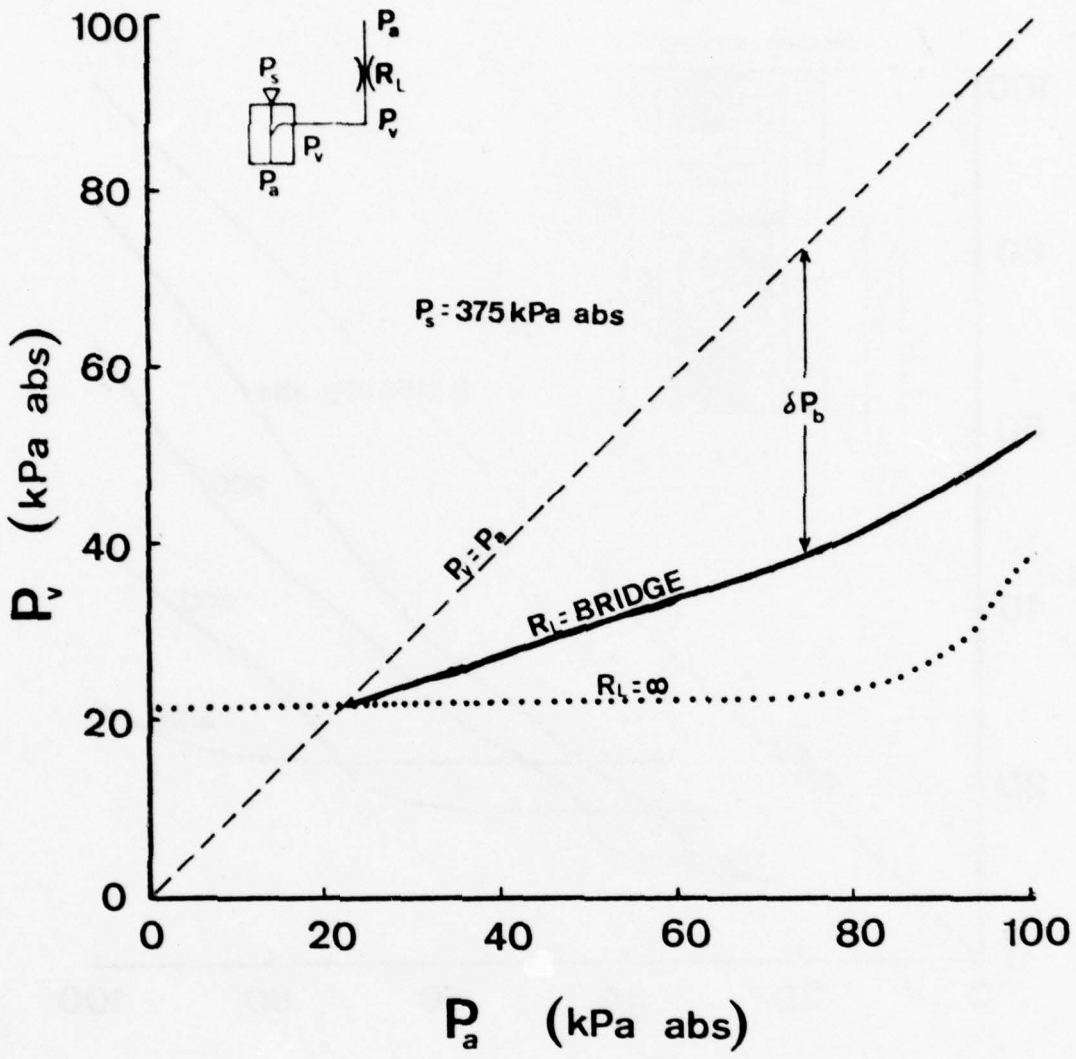

Figure 8. Absolute pressure characteristics of radial diffuser ejector with and without bridge loading (experimental).

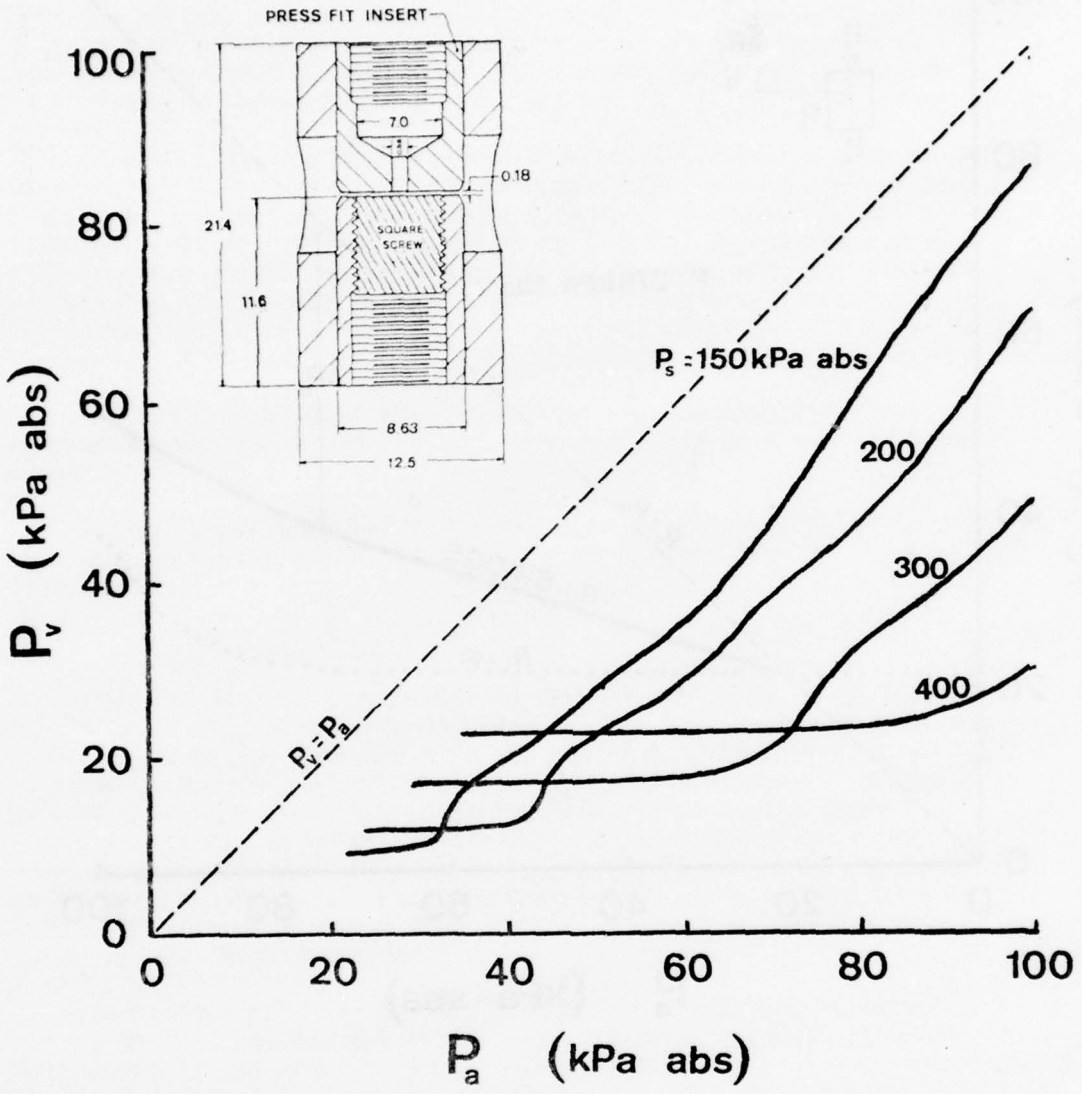

Figure 9. Absolute pressure characteristics of radial diffuser (experimental, dimensions in mm).

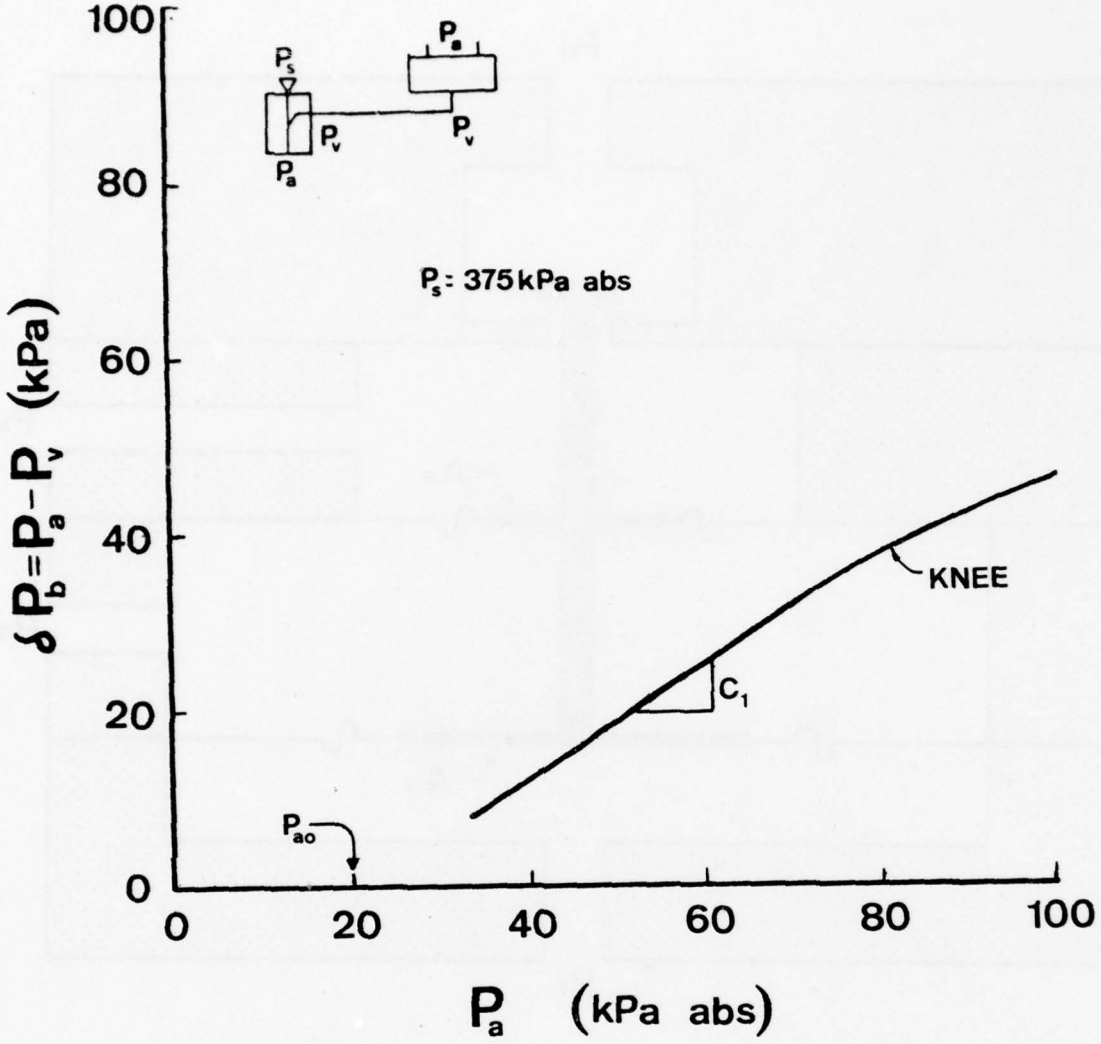

Figure 10. Bridge pressure drop characteristic with radial diffuser loaded with bridge (experimental).

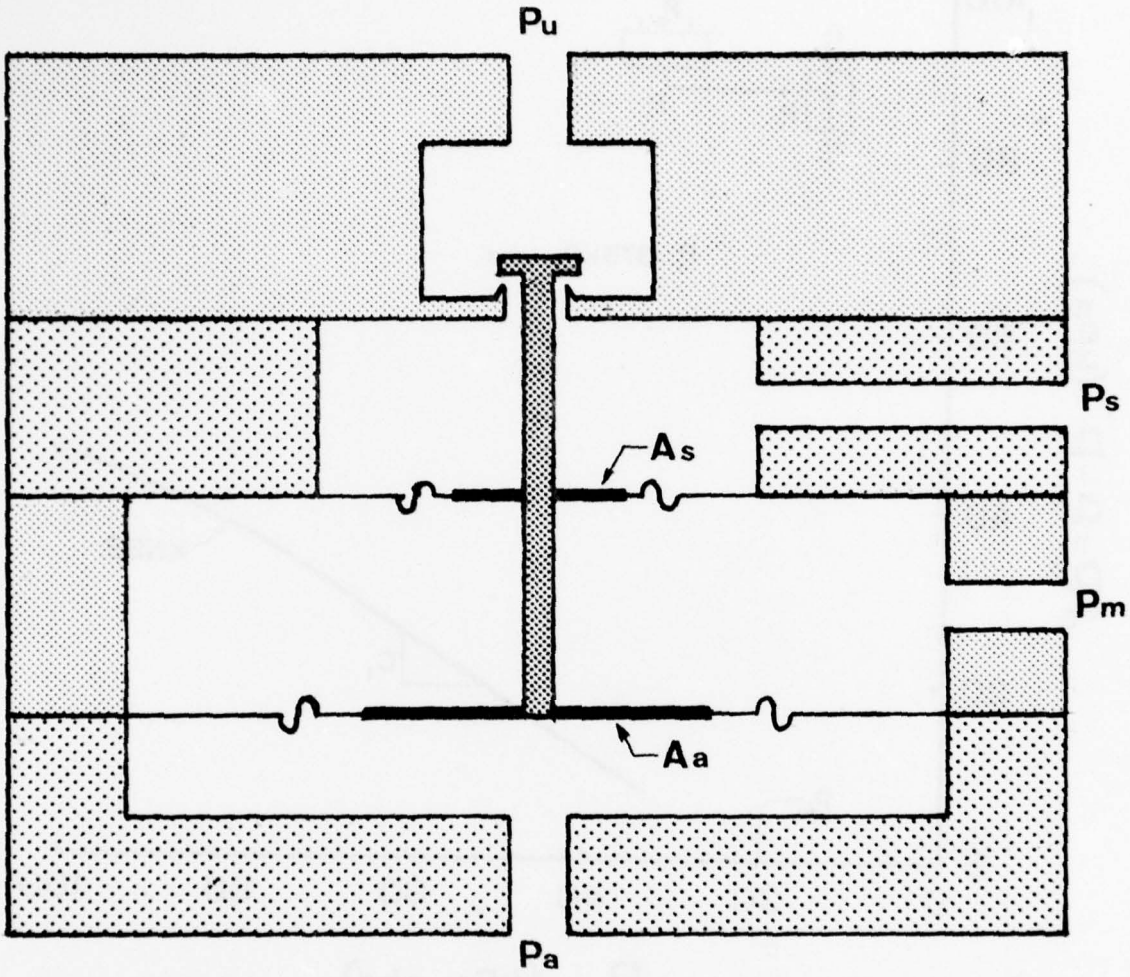

Figure 11. Schematic of ambient pressure scheduled pressure regulator.

is controlled by a flapper-valve type arrangement. The downstream side of the valve is the regulated pressure, P_s. Two diaphragms of different areas are provided. If the pressure intermediate to the diaphragms, P_m, were zero absolute, then the controlled pressure ratio from P_s to P_a would be equal to the area ratio A_a/A_s; however, this aneroid effect would require bellows and fabrication problems undesirable to our facilities. Thus, the intermediate pressure was elected to be driven by an ejector whose absolute pressure output would be a linear function of P_a if the ejector supply pressure is a linear function of P_a.

$$P_m = C_2 P_a \quad (\text{if } P_s \sim P_a) \tag{22}$$

Thus it can be shown that at a steady-state regulation point the regulated pressure, P_s, is linearly proportional to the ambient pressure, P_a.

$$P_s = \left[\frac{A_a}{A_s} + \left(1 - \frac{A_a}{A_s}\right) C_2 \right] P_a \tag{23}$$

The prototype regulator is built with an area ratio of 2.7 and the C_2 coefficient is observed to be 0.45. Thus the regulated pressure is 2.0 times P_a. The characteristics of the regulator and the ejector being driven by the regulator are given in a later figure. Notice that δP_b will now pass linearly through the origin ($P_{ao} = 0.0$).

Summary of Bridge-Type Sensor Equations

The bridge-type concentration sensor is analyzed in great detail in Appendixes A and B. The following equations summarize the results of the model (refer to Appendix A for nomenclature and functions).

$$\frac{\Delta P_o}{\delta P_b} = G_b S_b (X_s - X_{so}) \tag{24}$$

Where G_b is the gain function, θ is the sensor constant, S_b is the gas sensitivity coefficient, and X_{so} is an equivalent concentration to account for the sensor bridge asymmetry.

$$G_b = \frac{\sqrt{1 + 4\theta} - 2\theta - 1}{2\theta \sqrt{1 + 4\theta}} \tag{25}$$

$$\theta = \frac{b/a^2}{\mu^2/\rho} \delta P_b \tag{26}$$

When the compressible flow ejector is used to power the bridge, the bridge pressure drop becomes a function of ambient pressure as discussed in the preceding section (where C_1 and P_{ao} are constants).

$$\delta P_b = C_1(P_a - P_{ao}) \tag{27}$$

Substituting this into equation (24) yields the following:

$$\Delta P_o = G_b\, S_b\, C_1\, (X_s - X_{so})\, (P_a - P_{ao}) \tag{28}$$

Since density is a linear function of P_a, it can be seen that θ varies with the square of P_a (ρ_{SL} is sea level density, P_{SL} is sea level pressure).

$$\theta = \frac{b/a^2}{\mu^2/\rho_{SL}}\, C_1\, \frac{P_a}{P_{SL}}\, (P_a - P_{ao}) \tag{29}$$

With proper selection of θ, and P_{ao}, the sensor can be useful for measuring oxygen partial pressure over a limited range. The design approach is discussed in the following section. Ideally, $P_{ao} = 0$, and if $X_{so} = 0$, the equation reduces to the following (G_T is the combination of constants and functions).

$$\Delta P_o = G_b\, S_b\, C_1\, X_s\, P_a = G_T\, P_{as} \tag{30}$$

PERFORMANCE OF PROTOTYPE SENSOR

Some of the hardware used for this project was that used in a previous study concerning concentration and temperature sensing for life support systems. This work was performed by HDL for Brooks AFB in 1973 [6]. Refer to reference 6 for further details concerning the circuit layout and dimensions of sensors used in this study.

Bridge Design Guides

The theory and mathematical models for the bridge-type partial pressure sensor are derived in Appendix A and summarized in the preceding section. Some of the terms in the equation are fixed constants; some are adjustable parameters; and some are variables. The summarizing output equation is restated below.

$$\Delta P_o = G_b\, S_b\, C_1\, (X_s - X_{so})\, (P_a - P_{ao}) \tag{31}$$

In the terms, S_b is the gas sensitivity constant and is determined exclusively by the sample and reference gases used (S_b = 0.1045 for oxygen in air). C_1 is the slope of the δP_b versus P_a curve and is essentially constant depending upon the specific characteristics of the ejector design and the total resistance of the bridge relative to the ejector output resistance. C_1 is typically about 0.5. X_{so} is an equivalent concentration to account for bridge asymmetry. P_{ao} is the P_a axis intercept in which no positive pressure drop is developed across the bridge. P_{ao} is typically 35 kPa for the venturi-type and is 20 kPa for the radial ejectors at constant supply pressure. P_{ao} is 0 kPa with the scheduled pressure regulator. G_b is the sensor gain function which is a unimodal function of P_a. Over most of the operating range of principal concern, G_b varies but is greater than half of its peak value.

Selection of Sensor Operational Constants--The variation of G_b, and hence the selection of θ, is one of the major design variables of the sensor. As can be seen from Figure A-2 in Appendix A, G_b peaks at θ = 1.207. Thus the resistor's geometries should be designed so that G_b reaches its peak somewhere in the midrange between the two extremes of ambient pressures (altitudes) of major concern.

In Air Force applications, the crew can be exposed to cabin pressures ranging from 100 kPa (760 mm Hg) at sea level to 39 kPa (290 mm Hg) at 7,600 m (25,000 ft). Oxygen enrichment is not necessary to prevent hypoxia at altitudes below 1800 m (6,000 ft), and it is assumed that the probability of operation at such low altitudes is relatively low. Thus, pressures below 80 kPa (600 mm Hg) are considered more important and the sensor will be designed to give improved accuracy in the 40 to 80 kPa range. Hence θ^* = 1.207 (point at which G_b is maximum) should occur around Pa* = 60 kPa (Appendix C).

$$\theta^* = 1.207 = \frac{b/a^2}{\mu^2/\rho_{SL}} \frac{P_a^*}{P_{SL}} C_1 (P_a^* - P_{ao}) \tag{32}$$

The ratio μ^2/ρ_{SL} for air at STP is 2.817×10^{-13} kN; knowing C_1 and P_{ao} from ejector characteristics, allows computation of the ratio of geometric terms b/a^2 at the selected ambient pressure, P_a^*. Another useful relationship is the value of θ required at sea level for G_b to maximize at some P_a^*. The ratio of pressure drops can thus be stated.

$$\theta_{SL} = 1.207 \frac{P_{SL}}{P_a^*} \frac{(P_{SL} - P_{ao})}{(P_a^* - P_{ao})} \tag{33}$$

$$\frac{\delta P_N}{\delta P_L} = \frac{\sqrt{1 + 4\theta_{SL}} - 1}{2} \tag{34}$$

The placing of P_a^* in the midrange distributes the error due to G_b variations between low and high altitudes. If improved accuracy at either the high or low altitudes is required, P_a^* and hence the G_b peak can be shifted in that direction.

The second major nonlinearity arises from the ejector characteristic. As shown in Figures 6 and 8, P_{ao} increases as a linear function of ejector supply pressure. It is most desirable to have P_{ao} as low as possible so that partial pressure sensing will be more accurate at lower absolute pressures (higher altitudes); however, lowering P_s also lowers the knee of the ejector characteristic (point at which flow becomes choked and produces constant pressure). The lowered slope at the knee has a multiplicative effect upon the output: First, decreased δP_b will decrease the output directly, and secondly, it reduces G_b through θ.

The venturi-type ejector requires a supply pressure of about 150 kPa absolute for maximum δP_b at 80 kPa; however, P_{ao} is then about 35 kPa. A good trade-off with the radial flow ejector is with P_s = 400 kPa absolute in which P_{ao} = 20 kPa absolute is produced with only a slight knee effect around 90 kPa. When the venturi-type ejector is used with the scheduled regulator, the pressure ratio (of the ejector supply to ambient) should be large enough to just saturate the ejector. This requires a pressure ratio of about 2.0, and will produce a P_{ao} of 0 kPa absolute.

A third nonlinearity exists in the X_{so} term. If O_2 partial pressure is to be measured with a reference gas of air that is free of oxygen, no correction is required and X_{so} = 0 (or the bridge should be symmetrical). If O_2 is to be measured with ordinary air as a reference, then a bridge asymmetry equivalent to an X_{so} = 0.21 must be provided to account for the O_2 already present in air.

Flow and Contamination Considerations--Another trade-off exists concerning the physical sizing of the resistances. The smaller the geometry dimensions, the lower the required flow of analysis gases to the sensor. This is usually desirable; however, as the dimensions get smaller, the sensor becomes more vulnerable to contamination. Contaminant filtration is possible but is undesirable for two reasons: a contaminant filter adds resistance which could upset the resistance bridge balance, and it requires a dead space volume which will slow the sensor's response capability.

There are two considerations on the sensor's response time: the "purge time" which is equal to the volume (in the interconnecting tubing, etc. between the analysis gas source and the sensor) divided by the volumetric flow rate, and the time constant formed by the sensor's output resistance and the actuator's or pressure transducer's fluid

capacitance. The latter will have to be evaluated in the actual application but is no real consideration with the prototype system with the pressure transducer used.

The sensor's resistive coefficients can be written in normalized form so that the sensor constant, θ, and the flow rate can be selected independently.

$$\frac{K}{R^2} = \frac{b}{a^2} \frac{\rho}{\mu^2} = \frac{\theta}{\delta P_b} \tag{35}$$

where

$$\frac{b}{a^2} = \frac{1}{128\pi^2} \frac{1}{C_d^2} \left(\frac{d_e}{d}\right)^4 \left(\frac{A}{L}\right)^2 \tag{36}$$

(see Appendix A for nomenclature definitions).
The flow can be calculated using equations in Appendix A.

Expected Performance

The partial pressure of a gas is the product of its volumetric concentration (mole fraction) and the ambient pressure. An ideal partial pressure sensor would produce a family of linear curves passing the origin as shown in Figure 12.

The fluidic bridge gas partial pressure sensor evaluated in this report, using the model derived with typical constants[3], should produce the characteristics presented in Figure 13. These curves suffer from the offset P_{ao} and the nonlinearity due to G_b at both ends of the characteristics (P_a = 20 kPa and P_a = 100 kPa); however, the sensor does respond to both concentration and pressure, and should give very useful results in the range of 40 kPa (25,000 ft cabin altitude) to 100 kPa (sea level).

Experimental Results

The final sensor design was fabricated using discrete components rather than the laminates described in reference 6. It consists of metal etched laminates (from General Electric) for the laminar resistors, and plastic molded orifices (from Johnson Service) as shown in Figure 14. Different combinations of resistances were tried until sets of well-matched resistances were found that had the correct P_a*. The radial flow ejector was used to power the sensor. The results are shown

[3] θ= 2.05 at sea level (θ* = 1.207 at P_a* = 80 kPa), C_1 = 0.58, P_{ao} = 24 kPa, X_{so} = 0, gases = CO_2 in air (S_b = 1.056).

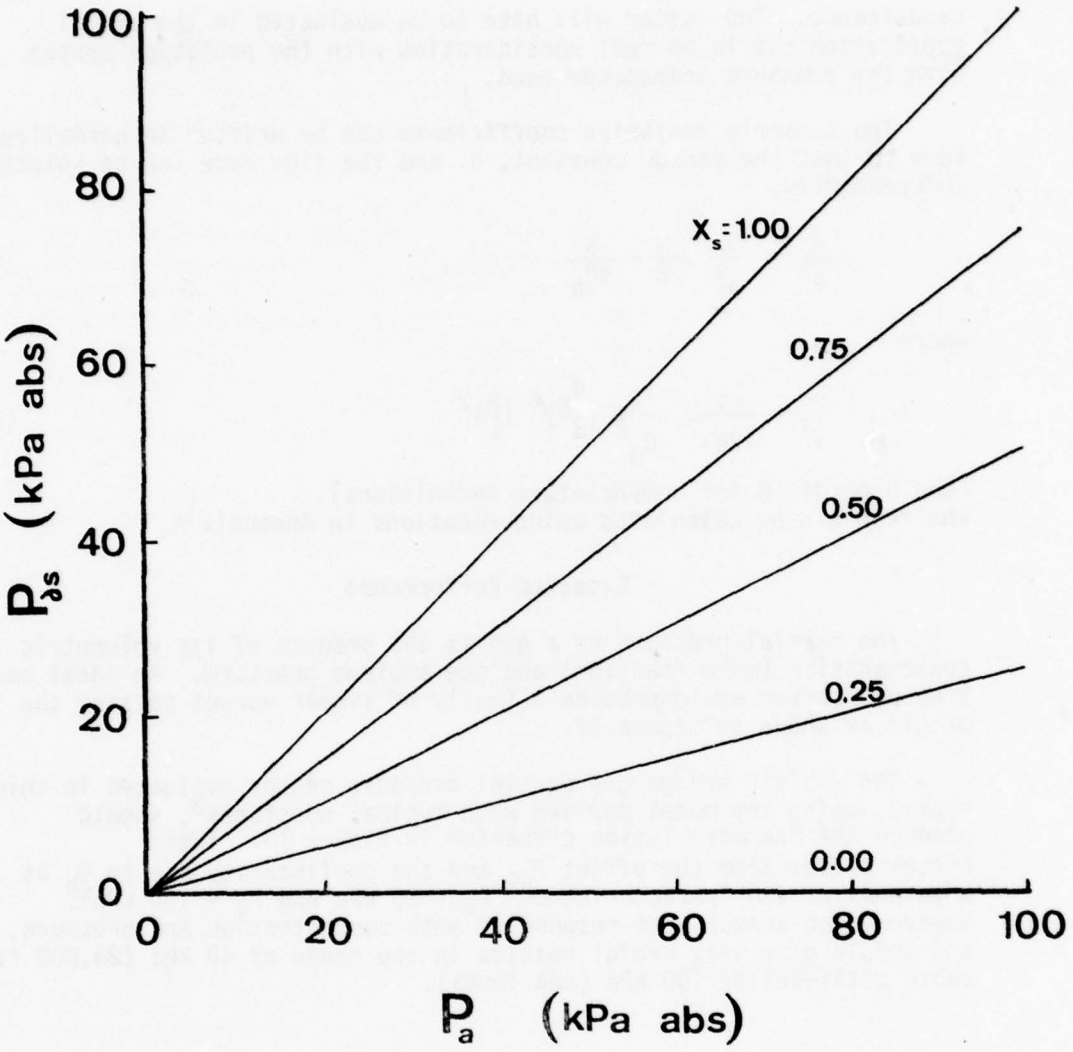

Figure 12. Ideal partial pressure sensor performance (hypothetical).

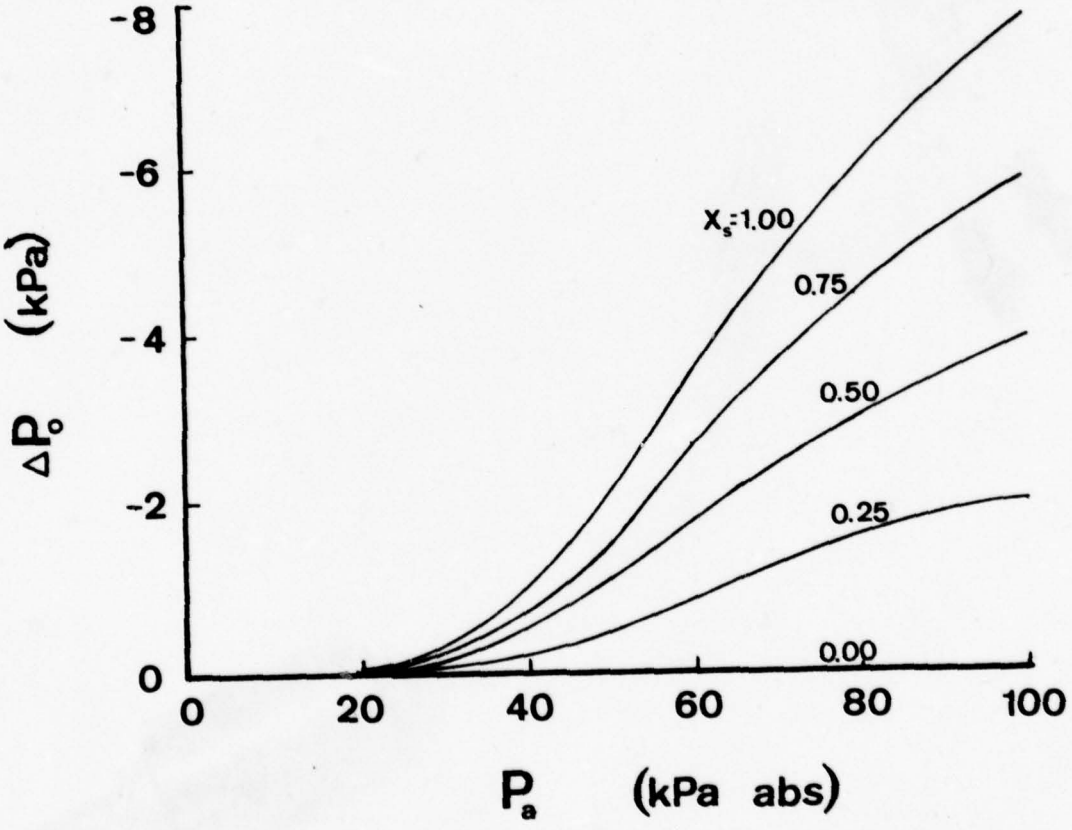

Figure 13. Expected partial pressure sensor performance with CO_2 in air (theoretical).

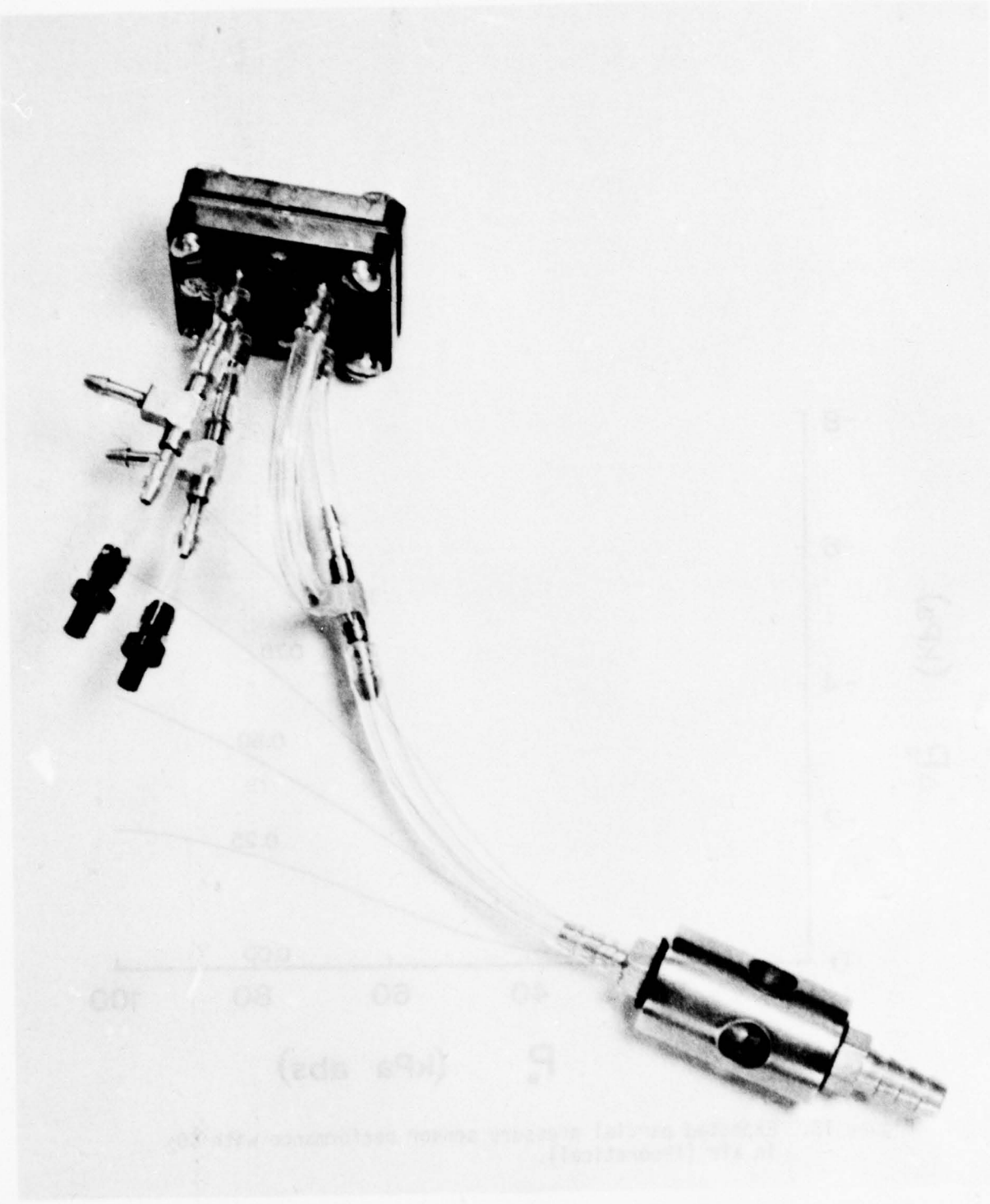

Figure 14. Prototype sensor hardware.

in Figure 15. This figure also shows the actual data taken with the x-y plotter which indicates the low noise exhibited by the signal. Since normal aircraft applications are in the range of 40 kPa to 80 kPa, the sensor is observed to be useful in that range.

The output signal shown in Figure 15 is lower than predicted. This signal degradation is a constant and is accurately explained by the nonideal analysis presented in reference 6. A detailed analysis has not been conducted in the present study, although the degradation factor appears to be about 0.4, and is indicated by the data shown in Figure 16.

At the conclusion of the project, a substantially improved sensor was constructed using the hardware from reference 6. This bridge has a sea level θ of 2.85 and a P_a^* of 65 kPa with the scheduled regulator. This sensor was powered with the scheduled pressure regulator discussed previously. The combination provided significantly improved results with larger outputs and improved linearity. The following data gives an indication of what can be expected from a second generation sensor. It is unfortunate that time did not permit a full evaluation of this sensor/regulator combination.

Figure 17 is the output of the improved Air Force sensor with the scheduled regulator. Notice that δP_b now goes through zero ($P_{ao} = 0$) and the sensor has improved characteristics in the 40 kPa to 80 kPa ambient pressure range.

The pressure-flow characteristics of this improved sensor are shown in Figure 18. The bridge is composed of the original orifices (after being hand matched) and two of the capillary resistors in parallel.

By comparison, the original sensor design described in reference 6 was tested for its ability to sense partial pressure. The results are shown in Figure 19. Notice from this plot that three design improvements could be made. First, the venturi-type ejector limits the δP_b characteristic both by C_1 and by P_{ao}. Secondly, G_b is designed to be maximum at sea level; thus the curves at lower pressure have decreased gain due to G_b. Thirdly, the null concentration curve is not zero but more importantly is not a straight line.

The undulations in the output curve with null concentration are very significant since this curve is added to the curves with fixed concentrations. The variations in the null curve are traceable to pressure-flow characteristics of the resistors in the bridge. The P-Q curve for the two resistors in the mixture and reference channels should be very closely matched for both the orifice and the capillary resistors; however, even if they are unmatched, one should look like a constant multiple of the other. If one curve has a variation where the other does not, a shift should occur in the output signal. The pressure-flow characteristics of the original design bridge are shown in Figure 20.

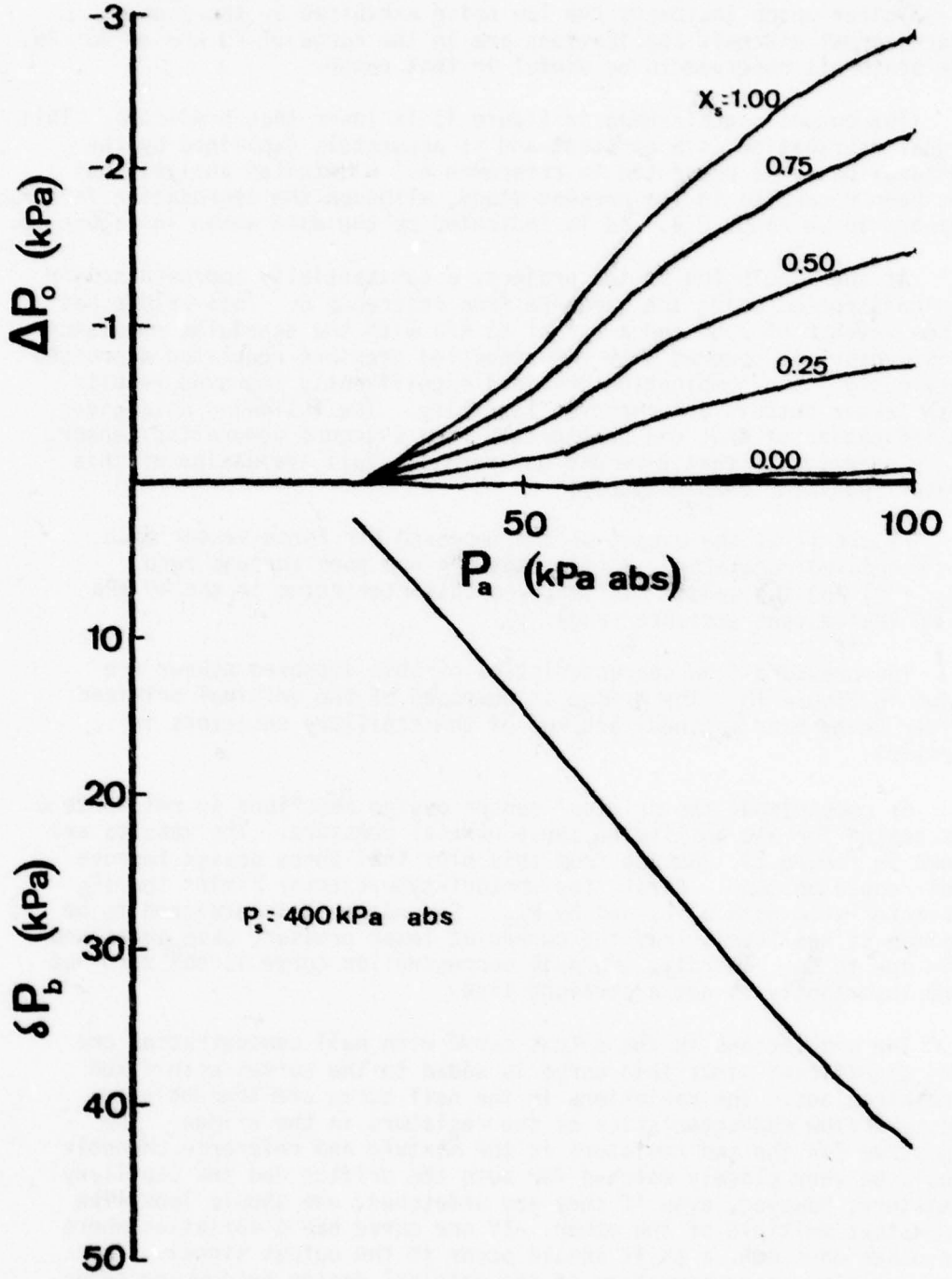

Figure 15. CO_2 sensing characteristics of discrete component prototype sensor with radial diffuser ejector (experimental).

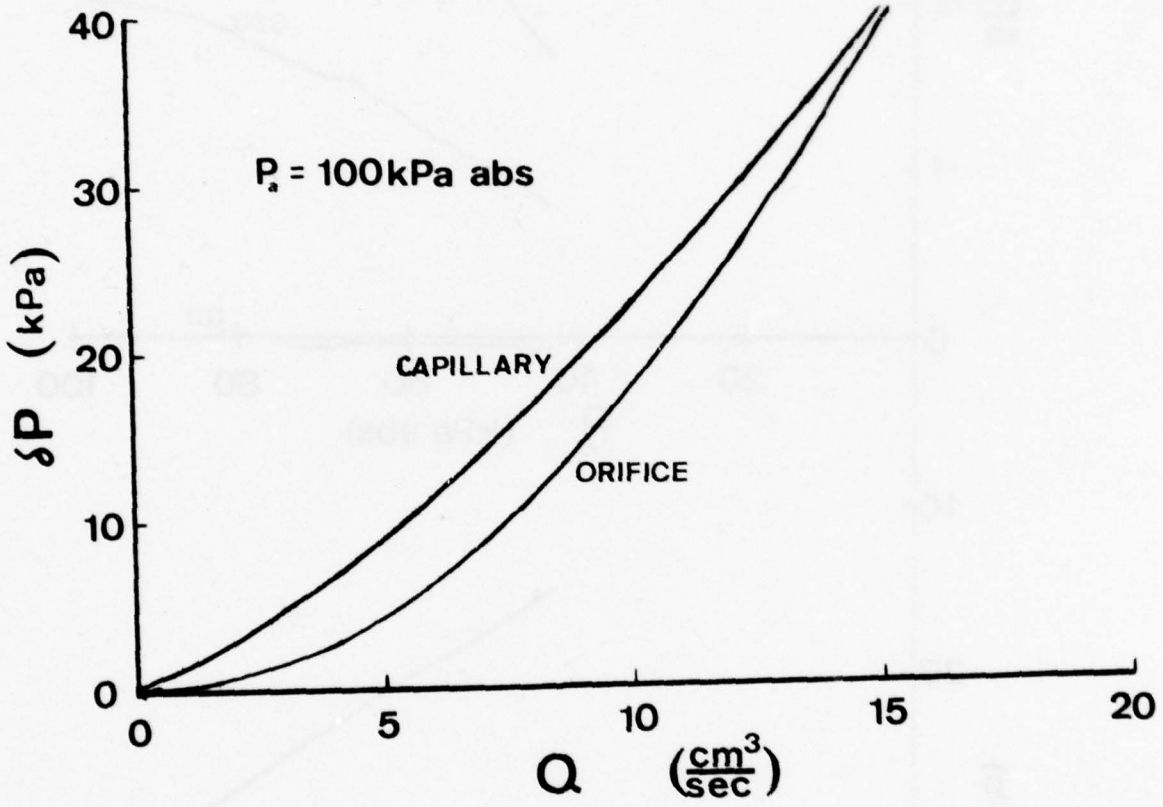

Figure 16. Pressure-flow characteristics of discrete prototype bridge resistors (experimental).

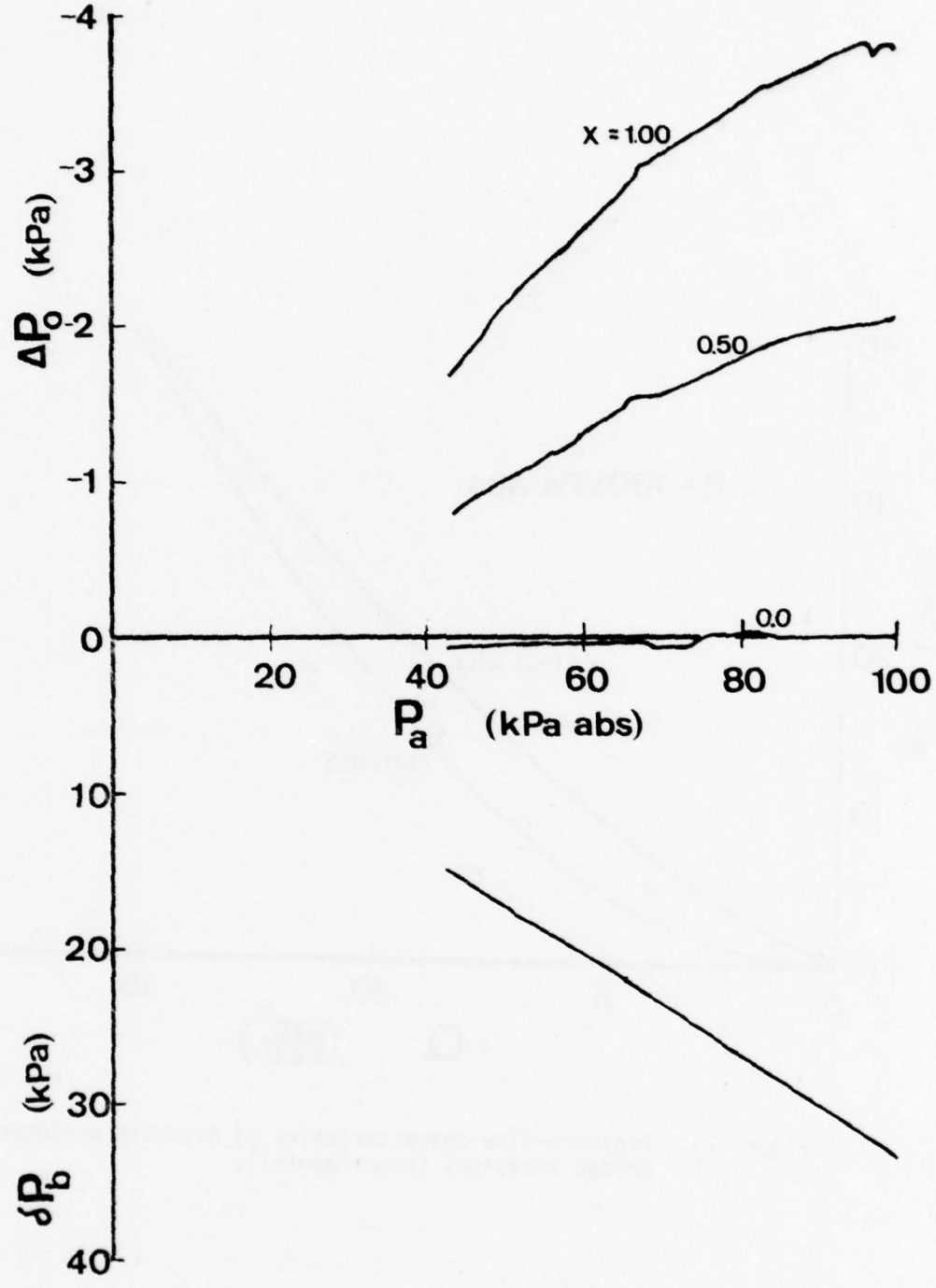

Figure 17. CO_2 sensing characteristics of the improved Air Force design with scheduled pressure regulator and venturi-type ejector (experimental).

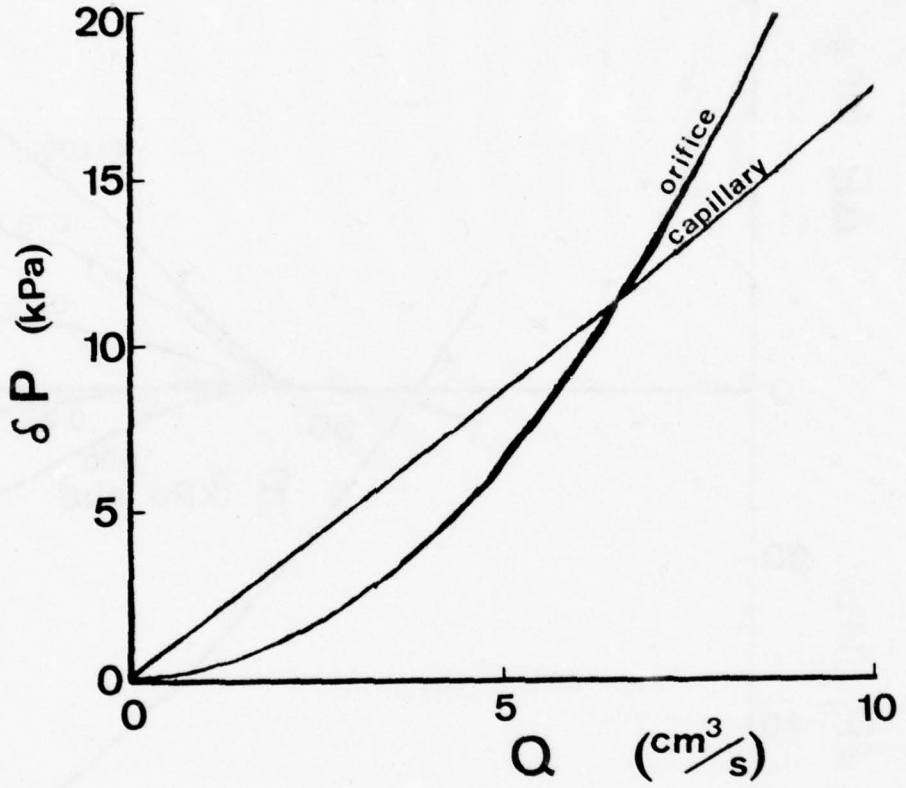

Figure 18. Pressure-flow characteristics of improved Air Force sensor (experimental).

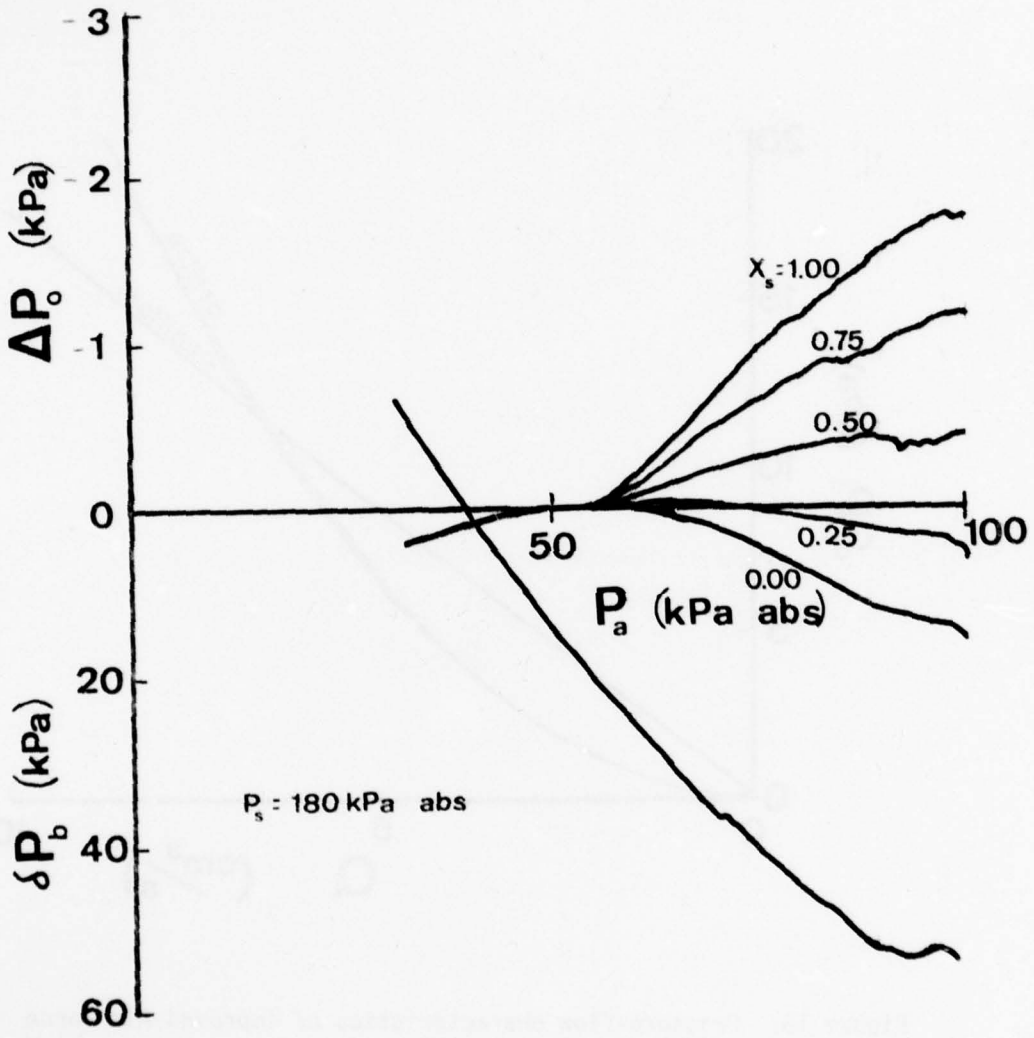

Figure 19. CO_2 sensing characteristics of original design with venturi-type ejector (experimental).

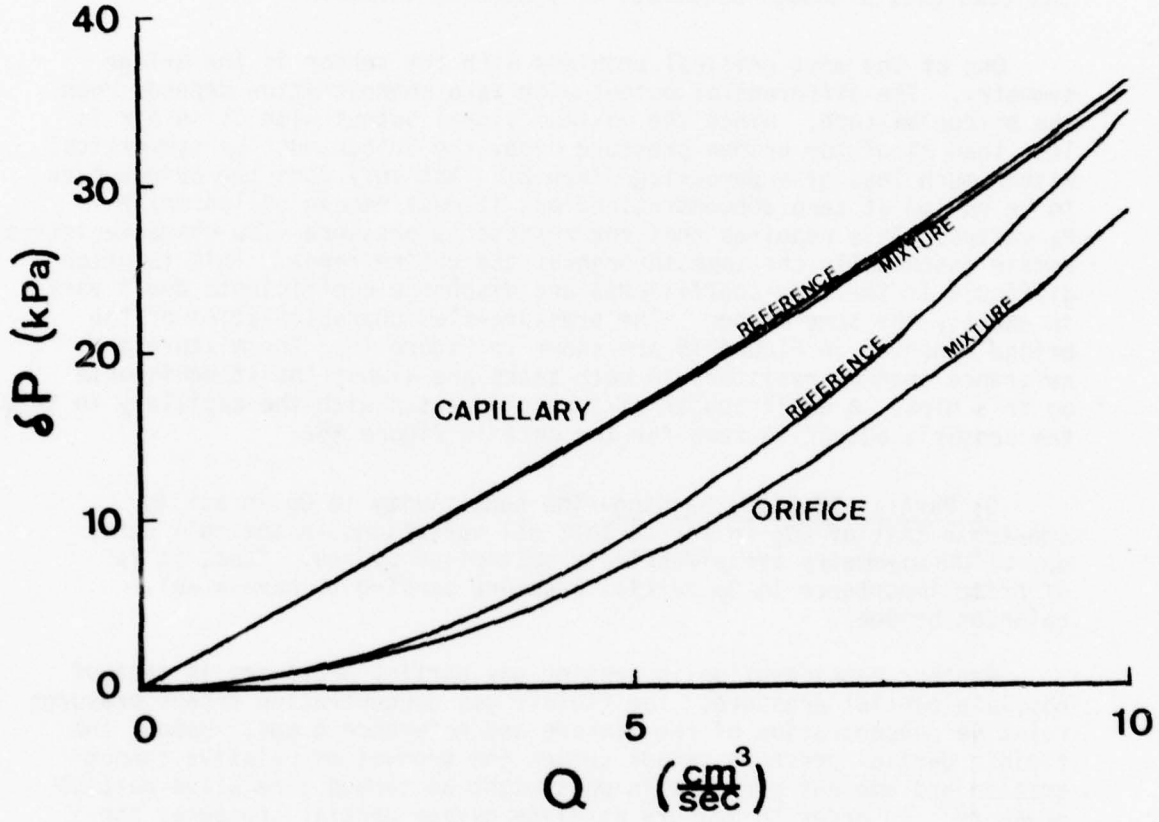

Figure 20. Pressure-flow characteristics of original design (experimental).

CO_2 Partial Pressure Sensing--Most of the experimental testing was conducted using CO_2 in air rather than O_2 in the air. This was done for two reasons: First, the sensor has a much larger signal output with CO_2 as compared to that with O_2, and secondly, there was less fire hazard with our oil sump vacuum pump. During most testing, the characteristic with zero concentration was of prime interest so that the test gas, although used, was of secondary concern.

One of the most critical problems with the sensor is the bridge symmetry. The differential output with zero concentration depends upon the bridge balance. Since the maximum signal output with O_2 in air is less than 2% of the bridge pressure drop, the bridge must be symmetrical within much less of a percentage than 2%. Not only does the bridge have to be nulled at zero concentration, but it must remain nulled while P_a varies. This requires that the resistor's pressure-flow characteristics remain essentially the same throughout the entire range. This is often difficult if the flow coefficients and discharge coefficients don't vary in exactly the same manner. The pressure-flow characteristics of the bridge reported in Figure 15 are shown in Figure 16. The mixture and reference channel resistors in both cases are almost indistinguishable on this plot. A small length of tubing was used with the capillary to trim the sensor's output to zero for the data in Figure 15.

O_2 Partial Pressure Sensing--The sensitivity to O_2 in air is one-tenth that of CO_2 in air so that all variations in the null curve due to the asymmetry are effectively multiplied by ten. Thus, it is of prime importance in O_2 partial pressure sensing to have a well-balanced bridge.

Another consideration in sensing gas partial pressures is that of absolute partial pressure. The fluidic gas concentration sensor measures relative concentration of the mixture and reference gases. Hence, the fluidic partial pressure sensor senses the product of relative concentration and ambient pressure in what might be termed a relative partial pressure. In order to measure absolute oxygen partial pressure, the bridge must be slightly unbalanced null concentration so that the output reading is 21% of the maximum output signal obtained with 100% O_2 (thus $X_{so} = 0.21$). This initial offset should then scale linearly to P_{ao}.

An offset to compensate for absolute partial pressure should be obtained by having the pressure-flow characteristics of the orifice and the capillary resistors differ by a constant multiple between the mixture and reference channels. Having only the orifice or capillary resistors unmatched should give undesirable results.

The discrete component bridge was trimmed by using various lengths of tubing on the capillary resistor until the null concentration signal was 21% of the 100% O_2 concentration signal at sea level. The sensor characteristics of O_2 in air with the 21% correction are shown in Figure 21.

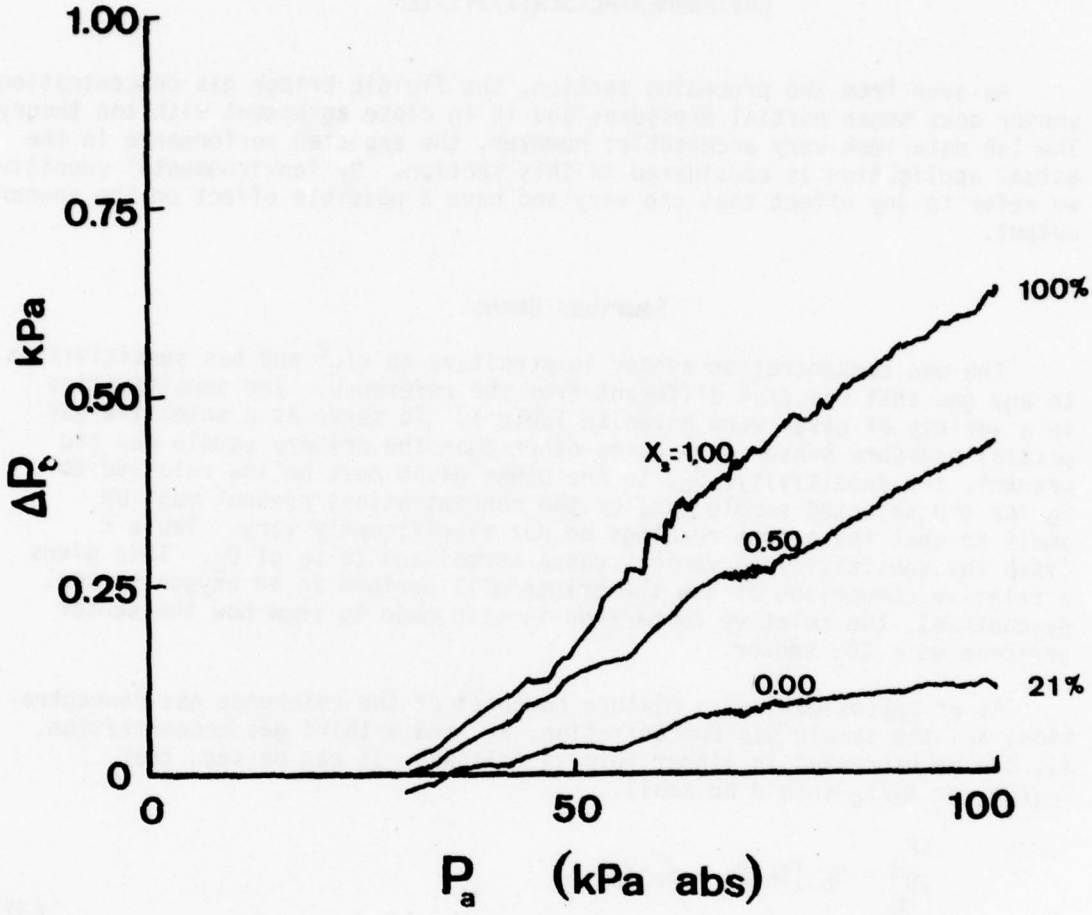

Figure 21. O_2 sensing characteristics of discrete component bridge with radial diffuser ejector (experimental).

ENVIRONMENTAL SENSITIVITIES

As seen from the preceding section, the fluidic bridge gas concentration sensor does sense partial pressures and is in close agreement with the theory. The lab data look very acceptable; however, the expected performance in the actual application is considered in this section. By "environmental sensitivity" we refer to any effect that can vary and have a possible effect on the sensor output.

Spurious Gases

The gas concentration sensor is sensitive to ρ/μ^2 and has sensitivities to any gas that has ρ/μ^2 different from the reference. The sensitivities to a variety of gases were given in Table 1. To serve as a selective gas partial pressure sensor when gases other than the primary sample gas are present, the sensitivity, S_b, to the other gases must be low relative to S_b for the selected sample gas, or the concentrations present must be small so that the output readings do not significantly vary. Table 2 lists the sensitivity to various gases normalized to S_b of O_2. This gives a relative comparison of how the bridge will perform as an oxygen sensor. By contrast, the relative comparison is also made to show how the sensor performs as a CO_2 sensor.

As an approximation, a mixture composed of the reference gas concentration, X_r, the sample gas concentration, X_s, and a third gas concentration, X_3, can be expressed in linear form as follows. It can be seen that S_{b3}/S_{bs} or X_3/X_s should be small.

$$\frac{\Delta P_o}{\delta P_b} = G_b \left[S_{bs}X_s + S_{b3}X_3\right] = G_b\, S_{bs}\, X_s \left[1 + \frac{S_{b3}\, X_3}{S_{bs}\, X_s}\right] \tag{37}$$

The form of the equation depends upon whether the third gas originates or is removed from the mixture. If a third gas is generated into an existing mixture of two gases, the ratio of the concentrations of the first gases remains fixed although their sum is reduced by the third gas.

The concentration sensor equation for a generated third gas into a constant mixture ratio can be stated as follows (primes designate the concentrations after the generation process; without primes designate original mixture before process).

$$\frac{\Delta P_o}{\delta P_b} = G_b \left[\, S_{bs}\, X_s(1-X_3') + S_{b3}\, X_3' \,\right] \tag{38}$$

TABLE 2. NORMALIZED SENSITIVITIES OF SELECTIVE GAS SENSOR

Sample	Reference	S_b/S_{bO_2}	S_b/S_{bCO_2}
O_2	Air	1.00	-0.10
CO_2	Air	-10.10	1.00
H_2O	Air	- 7.31	0.72
A	Air	1.55	-0.15
Ne	Air	10.97	-1.09
N_2	Air	- 0.53	0.05
CH_4	Air	- 2.71	0.27
C_2H_6	Air	-16.05	1.59
C_3H_8	Air	-28.54	2.83
C_4H_{10}	Air	-40.26	4.06
C_5H_{12}	Air	-53.89	5.34
C_8H_{18}	Air	-92.42	9.15

$$\frac{\Delta P_o}{\delta P_b} = G_b \, S_{bs} \, X_s \left[1 + \left(\frac{S_{b3}}{S_{bs}} + X_s \right) \frac{X_3'}{X_s} \right] \tag{39}$$

Thus the normalized sensitivity as well as the sample gas concentration determine how X_3 affects the output.

A third gas can be absorbed through chemical processing to remove its effect upon the sensor output. The model for an absorbed concentration, X_3, is stated as follows (same prime notation applies).

$$\frac{\Delta P_o}{\delta P_b} = G_b \, S_{bs} \, X_s' \tag{40}$$

$$= G_b \, S_{bs} \, \frac{X_s}{(1 - X_3)} \tag{41}$$

Notice that the third gas properties (or S_{b3}) have no effect upon the sensor's output; the third gas only affects the output by the volume it occupied.

Humidity

Respiratory gases are usually confronted with variations in humidity. It is assumed that water vapor can be treated as an ideal gas over the ranges of operation of interest to this project. If so, the gas sensitivity constant is 0.7639. This coefficient has been verified to be very close experimentally to this theoretical value. The concentration can be expressed as a function of the relative humidity ratio, ϕ, the saturation pressure at a given temperature, $P_{\partial SAT}$, and the ambient pressure, P_a.

$$X_{H_2O} = \frac{P_{\partial SAT}}{P_a} \, \phi \tag{42}$$

Assuming constant temperature operation at 25°C, $P_{\partial SAT}$ is 3.2 kPa. The preceding expression is plotted in Figure 22.

Typical Respiratory Mixtures

Exhaled respiratory gases can contain mixtures of oxygen, carbon dioxide, and water vapor. The partial pressures of these gases are assumed to have the following ranges: oxygen = 0 to 100 kPa; carbon dioxide = 0 to 8 kPa; water vapor = 0 to 6 kPa.

The validity of the linearized model has been verified using three constituent gases as well as two. Four constituent gases should also follow a linearized model.

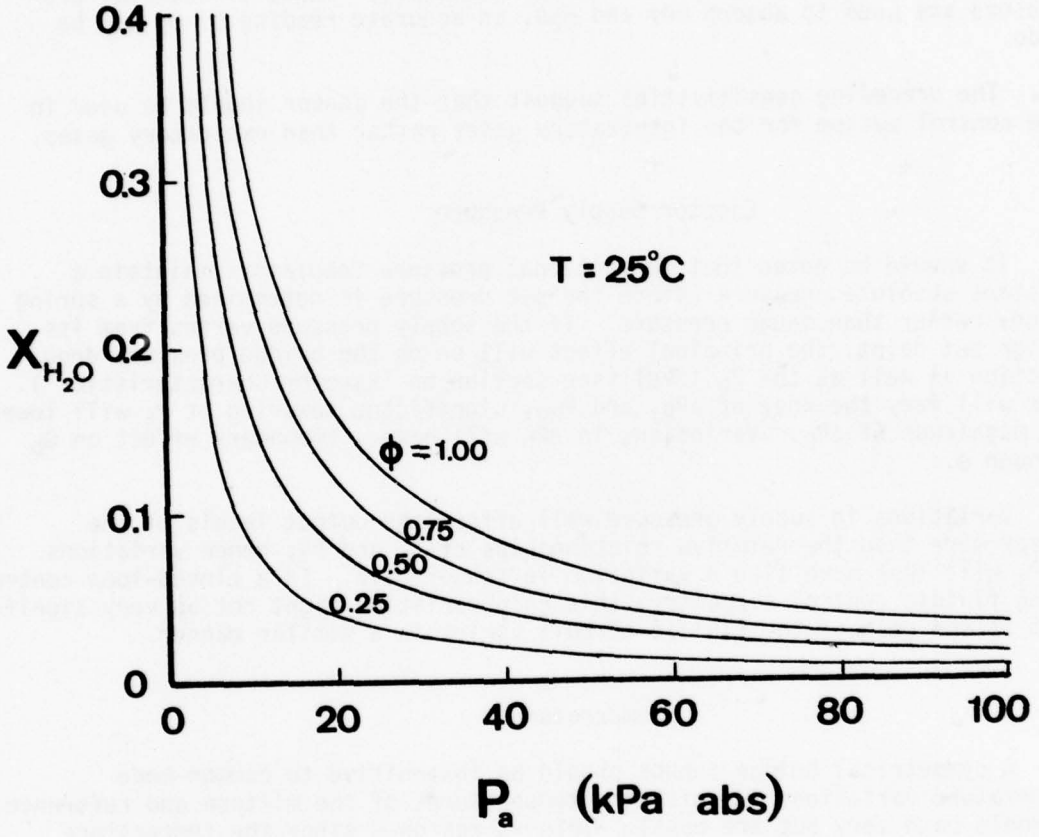

Figure 22. Water vapor concentration variation with relative humidity (theoretical).

The effect of the presence of variable amounts of CO_2 and H_2O generated in an O_2/air mixture can be seen in Figure 23. Ideally, these graphs should be flat, however, the slopes associated with the concentration of the third gas indicate that the O_2 sensor output will be greatly affected by the third gas.

Note that while the sensor is sensitive to a generated gas, it is insensitive to a third gas that has been absorbed. Thus, if chemical processors are used to absorb CO_2 and H_2O, an accurate reading of O_2 can be made.

The preceding sensitivities suggest that the sensor should be used in the control system for the inspiratory gases rather than expiratory gases.

Ejector Supply Pressure

It should be noted that conventional pressure regulators maintain a constant absolute pressure (since the set pressure is determined by a spring force) rather than gauge pressure. If the supply pressure varies from its design set point, the principal effect will be on the bridge pressure drop function as well as the P_b level (see section on "Ejector Characteristics"). This will vary the knee of δP_b, and P_{ao}; significant lowering of P_s will lower the magnitude of δP_b. Variations in δP_b will have a secondary effect on G_b through θ.

Variations in supply pressure will affect the output levels of the sensor more than the relative relationships of X_s and P_a; hence variations in P_s will look more like a variation in sensor gain. In a closed-loop control using fluidic control circuitry, this gain variation might not be very significant if the rest of the fluidic circuit varies in a similar manner.

Temperature

A symmetrical bridge sensor should be insensitive to common-mode temperature variations in which the temperatures of the mixture and reference channels both vary but are equal. This is reasoned since the temperature dependence of the viscosity of the mixture and reference gases usually have the same slope and both gases follow the ideal gas law; thus, μ^2/ρ should remain constant and thereby produce no concentration variation effect.

The ejector, however, might be temperature sensitive and produce a variation in δP_b with temperature which would affect the output signal. Further, although the resistive coefficient ratio remains constant, the bridge flow rate will vary with temperature, and, depending upon the ejector output resistance, the δP_b could vary due to this effect alone.

A slight temperature sensitivity is expected due to variations in δP_b. This sensitivity has been evaluated in preliminary data to be very small. The original design bridge was used with the radial flow ejector (ΔP_o = -0.15 kPa, δP_b = 7 kPa, G_b= -0.0652 @ 7 kPa, ΔT = 45°C).

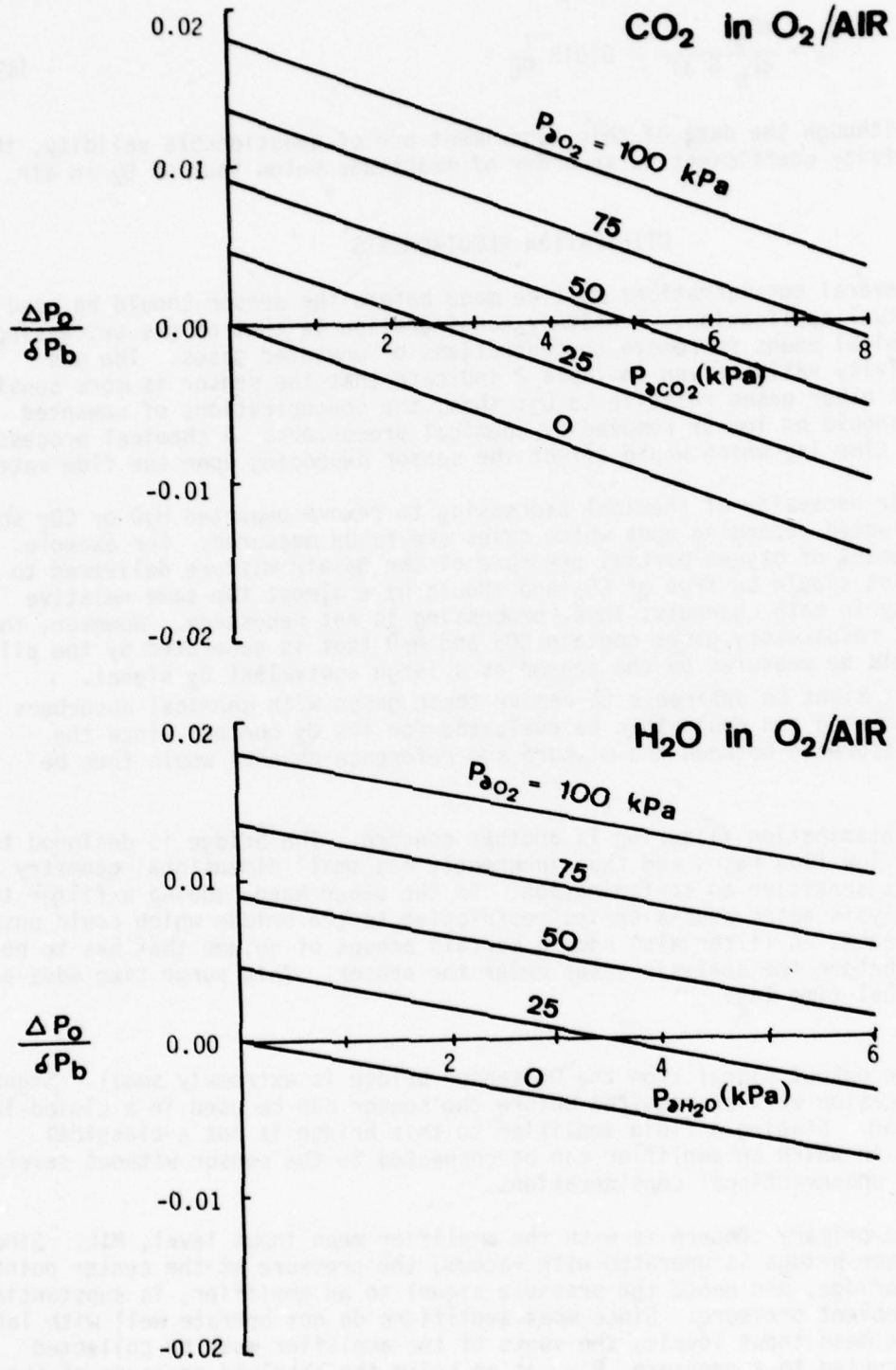

Figure 23. O_2 sensor sensitivity to CO_2 and H_2O (theoretical).

$$S_\theta = \frac{\Delta P_o}{\delta P_b \; G \; \Delta T} = 0.013 \; \frac{1}{^oC} \qquad (43)$$

Although the data of this experiment are of questionable validity, this sensitivity coefficient is an order of magnitude below that of O_2 in air.

UTILIZATION REQUIREMENTS

Several considerations must be made before the sensor should be used in the actual application. A primary consideration is that of gas processing by chemical means to remove concentrations of unwanted gases. The gas sensitivity ratios given in Table 2 indicate that the sensor is more sensitive to most other gases relative to O_2; thus, the concentrations of unwanted gases should be low or removed by chemical processors. A chemical processor adds a time lag which would affect the sensor depending upon the flow rate.

The necessity of chemical processing to remove unwanted H_2O or CO_2 should be evaluated depending upon which gases are to be measured. For example, measurement of oxygen partial pressure of the O_2-air mixture delivered to the pilot should be free of CO_2 and should have almost the same relative humidity in both channels; thus, processing is not necessary. However, the exhaled respiratory gases contain CO_2 and H_2O that is generated by the pilot, and would be measured by the sensor as a large equivalent O_2 signal. Thus, it might be desirable to remove these gases with chemical absorbers. The resulting gas could then be evaluated for its O_2 content since the only difference between the mixture and reference channel would then be the O_2.

Contamination filtering is another concern. The bridge is designed to require low flow rates and thus inherently has small dimensional geometry which is sensitive to contamination. On the other hand, adding a filter to the analysis gases adds a series restriction to the bridge which could upset the balance. A filter also adds a certain amount of volume that has to be purged before the analysis gases enter the sensor. This purge time adds an additional time lag.

The output signal from the O_2 sensor bridge is extremely small. Signal amplification will be required before the sensor can be used in a closed-loop regulator. Staging a fluid amplifier to this bridge is not a classical problem in which an amplifier can be connected to the sensor without several special unconventional considerations.

The primary concern is with the amplifier mean input level, MIL. Since the sensor bridge is operated with vacuum, the pressure at the center point in the bridge, and hence the pressure signal to an amplifier, is substantially below ambient pressure. Since most amplifiers do not operate well with large negative mean input levels, the vents of the amplifier must be collected and evacuated to a pressure, P_{va}, at or below the absolute pressure of the center point of the bridge, P_o. See Figure 24.

$$MIL = \frac{(P_{om} - P_{va}) + (P_{or} - P_{va})}{2} \qquad (44)$$

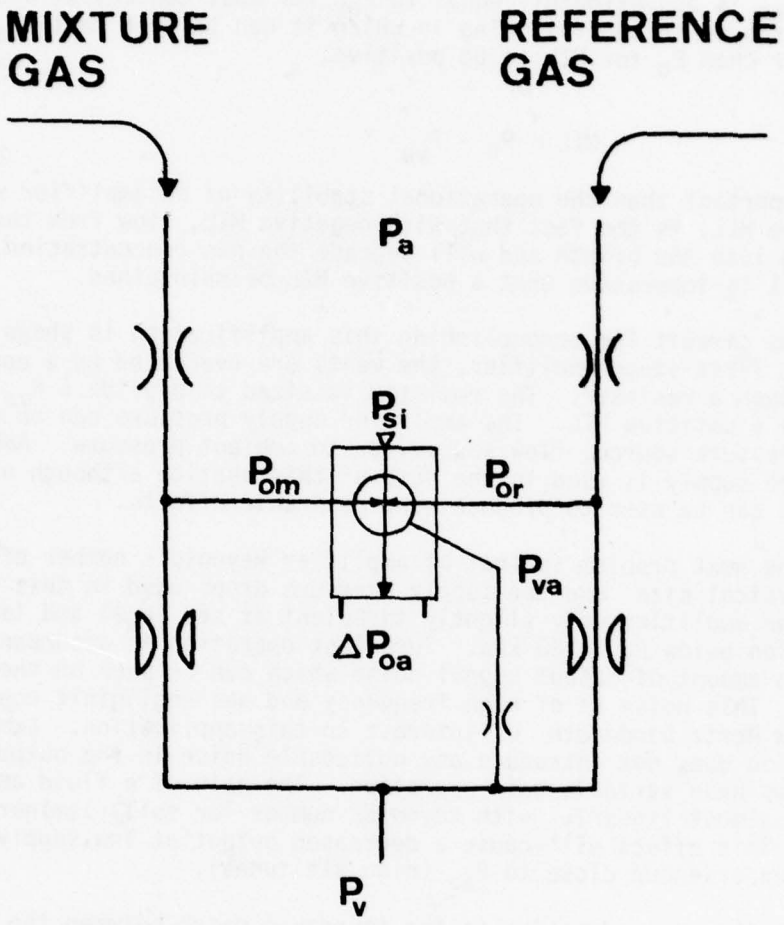

Figure 24. Circuit schematic of sensor bridge with amplifier.

Since P_{om} is approximately equal to P_{or} for most concentrations, mean input reduces to the following in which it can be seen that P_{va} should be lower than P_o for MIL to be positive.

$$MIL = P_o - P_{va} \tag{45}$$

More important than the operational stability of an amplifier with positive MIL, is the fact that with negative MIL, flow from the amplifier will go into the bridge and will degrade the gas concentration information. Thus, it is imperative that a positive MIL be maintained.

The circuit for accomplishing this amplification is shown in Figure 24. In this first stage amplifier, the vents are evacuated by a connection to P_v through a resistor. The resistor is sized to provide a P_{va} that will produce a positive MIL. The amplifier supply pressure can be connected to a pressure source, flow source, or to ambient pressure. Ambient pressure supply is used in the data of this section although other supply sources can be used to produce more desirable effects.

The next problem is that of amplifier Reynold's number effects. The physical size and the supply pressure drops used in this application make the amplifier only slightly turbulent at sea level and laminar for operation below $P_a \approx 80$ kPa. Turbulent operation is accompanied with a certain amount of output signal noise which can be seen on the signal trace. This noise is of high frequency and has negligible content below the few hertz bandwidth of interest to this application. Laminar operation does not introduce any noticeable noise in the output signal but does have variable gain operation. The gain of a fluid amplifier varies almost linearly with Reynolds number for fully laminar operation [10]. This effect will cause a decreased output at low supply pressure drops experienced close to P_{ao} (high altitudes).

Another consideration is the impedance match between the sensor's output resistance, R_{os}, and the amplifier's input resistance, R_{ia}. The staged pressure gain of the amplifier is given as a function of the infinite load impedance pressure gain, $G_{p\infty}$, and the impedance ratio.

$$G_p = \frac{G_{p\infty}}{1 + \frac{R_{os}}{R_{ia}}} \tag{46}$$

If $R_{os}/R_{ia} = 0$, the maximum pressure gain is achieved, if $R_{os}/R_{ia} = 1.0$, the maximum power gain is obtained, and if $R_{os}/R_{ia} = \infty$, the maximum flow gain is realized.

Generally the purpose of a first stage amplifier is to provide a buffer and signal conditioning preferably with a gain between maximum pressure and maximum power loading. Thus, for a given bridge and hence a given R_{os}, the amplifier input impedance should be sized to be equal to or greater than R_{os}.

The output characteristics of the sensor bridge are given in Figure 25 from which the output resistance can be calculated as 1.7 M lohm.[4] The amplifier used in this study is a single G.E. laminate whose characteristics are given in Figure 26. The input resistance of the amplifier is about 1.3 M lohm and the infinite load impedance pressure gain of the amplifier is 10. Thus, the expected pressure gain as staged is 4.1. Figure 27 is the amplifier transfer characteristics at infinite load impedance from which good linearity and $G_{p\infty} = 10$ can be observed.

Figure 28 illustrates the sytem output (CO_2 in air) with one stage of amplification on the bridge (P_v = 50 kPa abs, P_{va} = 82 kPa abs, MIL = 82 kPa abs, and $P_{si} = P_a$). Notice in comparison with Figure 15, that a gain of 4.5 has been achieved and the output impedance has been changed from the 1.7 M lohm of the bridge to the 1.5 M lohm of the amplifier and good isolation has been achieved.

The mean output level (MOL) of the amplifier is now 89 kPa abs whereas it was 83 kPa abs for the bridge. One more stage of amplification can achieve a signal having sufficient gain and MOL to be used in conventional altitude compensation circuits.

Figure 29 shows the amplifier signal output using O_2 in air with the absolute partial pressure compensating offset in the output. Notice the signal noise level change in going from laminar to turbulent which occurs around P_a = 70 kPa abs. Notice also the decreased output in the vicinity of P_{ao} due to the loss of amplifier gain at low Reynolds number.

The first amplifier was staged with almost no difficulty as long as the mentioned considerations were taken into account. It will be less trouble to stage a second amplifier onto the circuit so that the signal can be used in conventional fluidic circuits.

---

[4] The unit of measure of a linear fluid resistor is termed a lohm (linear ohm) and is equal to a kN sec/m^5. Note that 1.0 kPa per cm^3/sec is 10^6 lohm, or 1 M lohm.

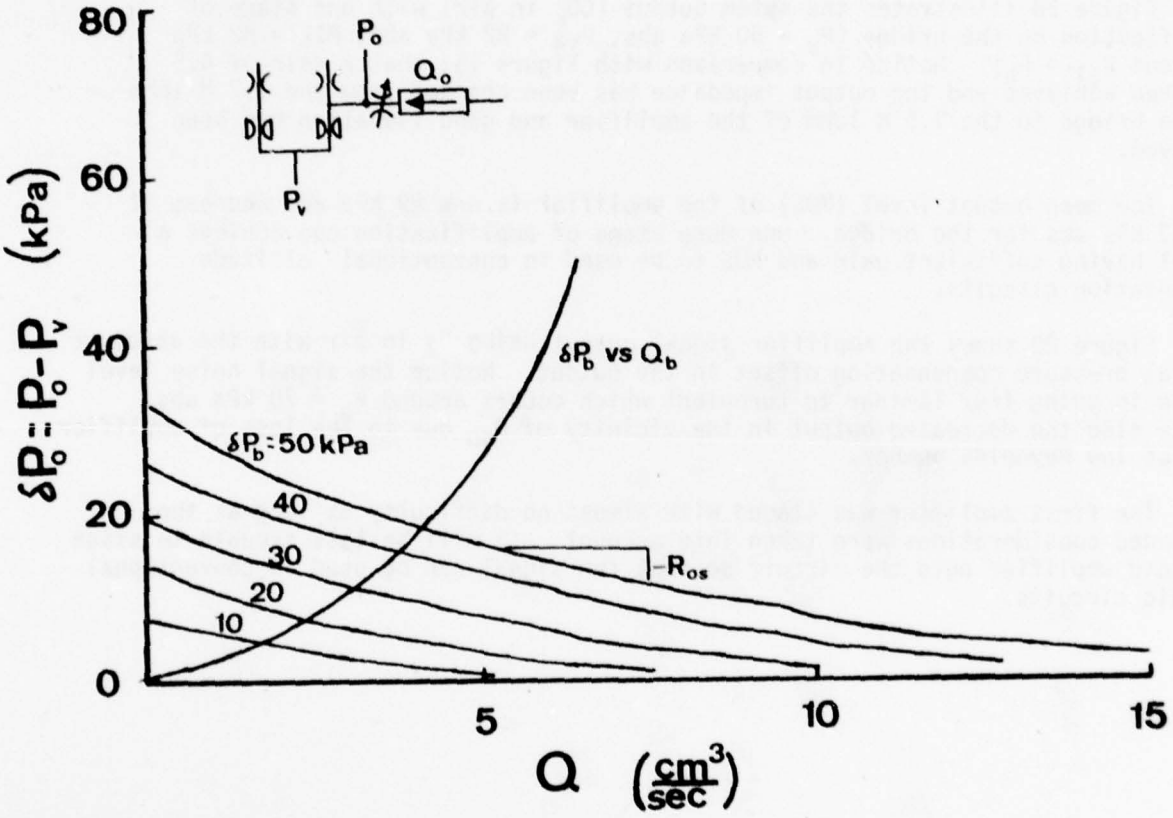

Figure 25. Output characteristics of discrete component sensor bridge (experimental, Q uncompensated to STP).

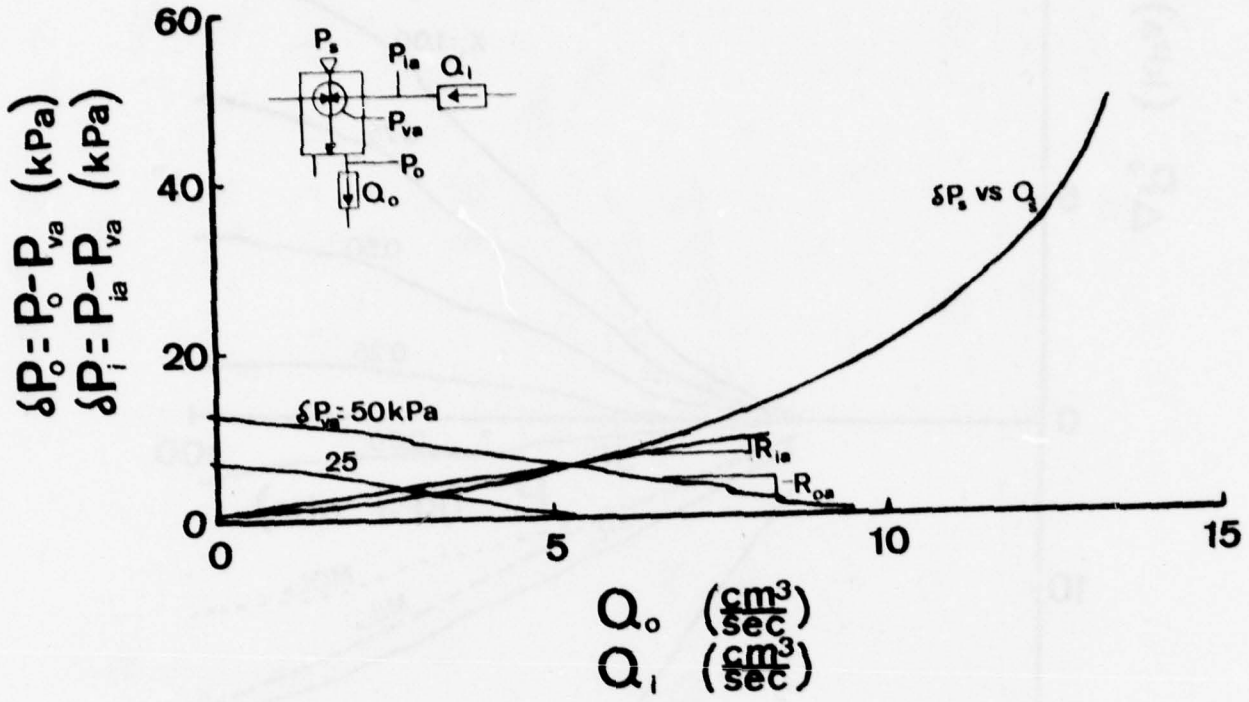

Figure 26. Amplifier characteristics (experimental).

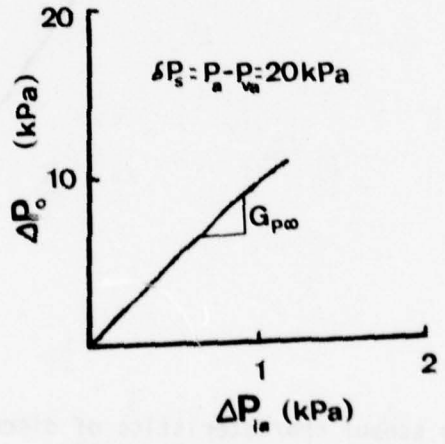

Figure 27. Amplifier transfer characteristics (experimental, infinite load impedance).

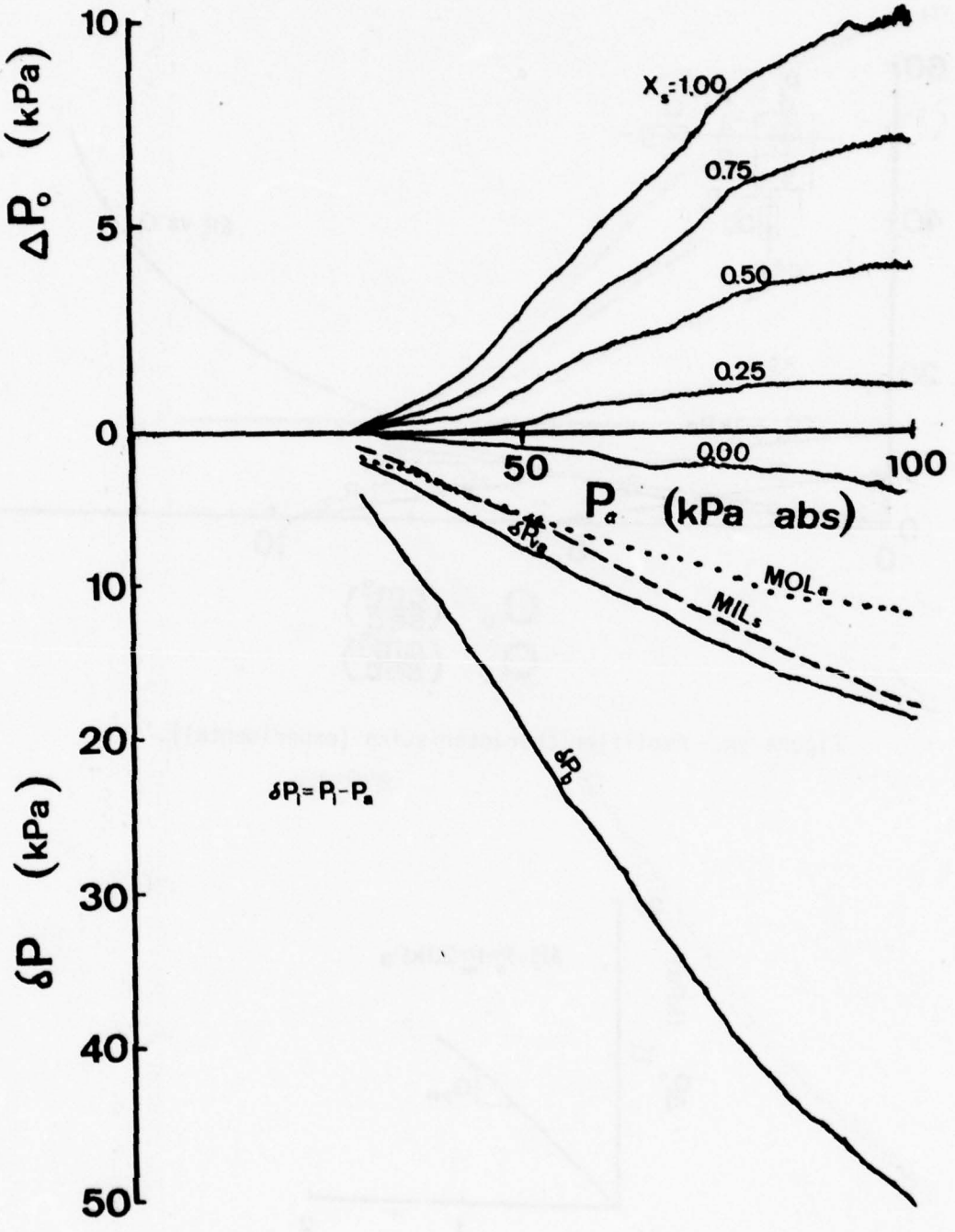

Figure 28. CO_2 sensor characteristics of discrete component bridge with amplifier (experimental).

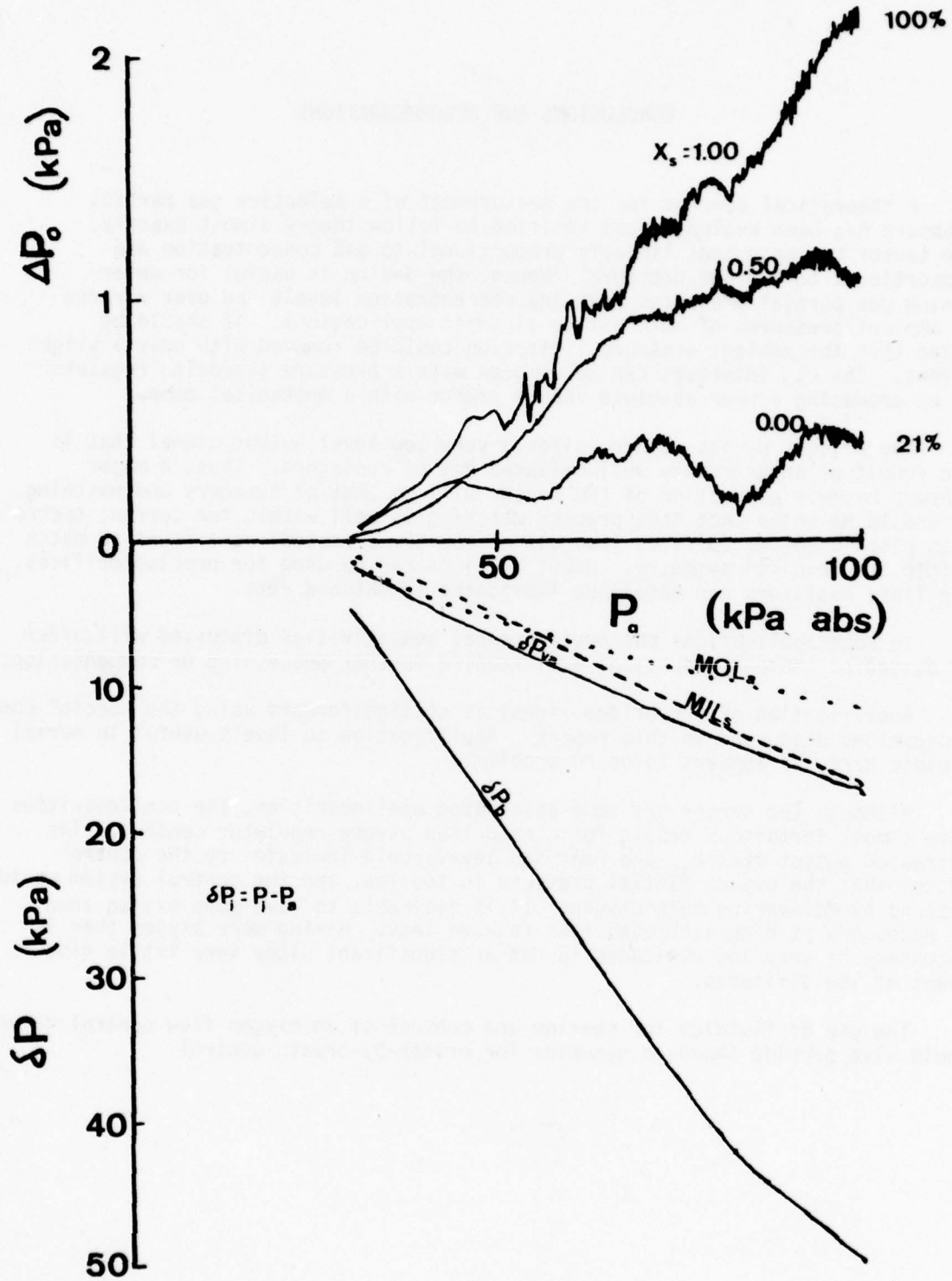

Figure 29. 02 sensor characteristics of discrete component bridge with amplifier (experimental).

CONCLUSIONS AND RECOMMENDATIONS

A theoretical concept for the measurement of a selective gas partial pressure has been evaluated and verified to follow theory almost exactly. The sensor has an output linearly proportional to gas concentration and proportional to ambient pressure. Hence, the device is useful for determining gas partial pressures over any concentration levels and over a range of ambient pressures of interest to aircraft applications. It should be noted that the ambient pressure limitation could be removed with only a slight effort. The P_{ao} intercept can be removed with a pressure scheduled regulator or by producing a near absolute vacuum source with a mechanical pump.

The bridge, by its nature, gives a very low level output signal that is the result of an extremely well-balanced set of resistors. Thus, a major concern in mass production of the sensor will be that of symmetry and matching. It should be noted that this precise matching is well within the current technology. Even plastic molded orifices (two out of the three tested) were found to match within the required symmetry. Jewel bearings can be used for precise orifices. Capillary resistors can easily be fabricated in matched sets.

In some applications the environmental sensitivities discussed will offer no obstacle. Some applications will require further processing or compensation.

Amplification of the bridge signal is straightforward using the special considerations discussed in this report. Amplification to levels useful in normal fluidic circuits appears to be no problem.

Although the sensor has some associated nonlinearities, the nonlinearities have a most fortuitous result for closed-loop oxygen regulator control. The decreased output near P_{ao} and near sea level would indicate to the control system that the oxygen partial pressure is too low, and the control system would respond by delivering more oxygen. It is desirable to have more oxygen than is necessary at high altitudes than to have less. Having more oxygen than is necessary at very low altitudes is not as significant since very little time is spent at low altitudes.

The use of fluidics for sensing and control of an oxygen flow control valve could also provide improved dynamics for breath-by-breath control.

ACKNOWLEDGMENTS

A special thanks is due to Captain Paul Zalesky, Captain Tom Morgan, and Captain Richard Stribley, who served as technical monitors, and to Dr. Billy Richardson, Dr. E. G. Shaw, and staff at the USAF School of Aerospace Medicine for their interest in the concept.

Mr. Vee Sridharan served as Graduate Research Assistant during the major portion of the project. Mr. Steve Mhoon, UTA Research Assistant, vitally helped with the final design and data. Mr. Rob Auld helped with technical assistance and graphics. Mrs. Alice Kennedy, UTA, excelled in typing and clerical support. Mr. Bill Hutchinson, UTA, edited the report submitted to USAFSAM. Appreciation is also expressed to the UTA staff for their interest and support.

REFERENCES

1. Campagnuolo, C. J., and H. C. Lee. Review of some fluid oscillators. Report No. HDL-TR-1438, U.S. Army, Apr 1969.

2. Cox, B. M. Fluidic air-fuel ratio sensor. Paper No. 74-Pet-21, ASME, New York, Sept 1974.

3. Farber, E. A., et al. Hydrogen and oxygen sensor development. Final Report under NASA Contract No. NAS 10-1255 Mod. 25, University of Florida, 31 Oct 1972.

4. Greenspan, L. An oxygen partial pressure warning instrument. J Res Natl Bur Std 67C No. 1, Jan to Mar 1963.

5. Joyce, J. W., and R. L. Woods. A flueric gas-concentration sensor for diver breathing gases. Proceedings, 1973 Divers' Gas Purity Symposium, Columbus, Ohio, 27-28 Nov 1973.

6. Joyce, J. W., and R. L. Woods. Fluidic sensors for life support systems. Report No. HDL-TM-75-17, U.S. Army, 1975.

7. Kirshner, J. M., and A. E. Schmidlin. Fluidic sensors. Proceedings of the HDL State-of-the-art Fluidics Symposium, U.S. Army, Nov 1974.

8. LeRoy, M. J., and S. H. Gorland. Molecular weight sensor. Instruments and control systems, pp. 81-82, Jan 1971.

9. Macia, N. F., and R. L. Woods. A model for the fluidic port characteristic of ejectors. Paper was presented at the 1976 Winter Annual Meeting, ASME, New York, Dec 1976.

10. Manion, F. M., and G. Mon. Design and staging of laminar proportional amplifiers. HDL-Tr-1608, Harry Diamond Labs, Adelphi, Md. Sept 1972.

11. Ostdiek, A. J., and F. M. Manion. Instrument for measurement of fluid density or composite fluid mixing ratio. U.S. Patent No. 3,765,224, 16 Oct 1973.

12. Prokopius, P. R. A fluidic device for measuring constituent masses of a flowing binary gas mixture. NASA TM X-2741, Cleveland, Ohio, Mar 1973.

13. Villarroel, F. Analog flueric gas concentration sensor, U.S. Patent No. 3,771,348, 13 Nov 1973.

14. Villarroel, F., and C. W. Ragsdale. Army CO_2/O_2 concentration monitor. Report No. HDL-TM-7131, U.S. Army, Dec 1971.

15. Villarroel, F., and R. L. Woods. Analog flueric gas concentration sensor. Report No. HDL-TM-73-9, U.S. Army, June 1973.

16. Wilke, C. R. A viscosity equation for gas mixtures. J Chem Phys. Vol. 18, No. 4, Apr 1950.

17. Woods, R. L. Fluidic partial pressure sensor. U.S. Patent No. 4,008,601, 22 Feb 1977.

18. Woods, R. L., and F. Villarroel. A fluidic bridge gas concentration sensor applicable to respiratory gases. J Dyn Sys Meas and Control, Sept 1975.

APPENDIX A

DERIVATION OF BRIDGE SENSOR EQUATION

Gas Concentration Sensor Equation

The bridge-type gas concentration sensor is composed of a symmetrical 4-way bridge as shown in Fig. A-1. Each channel of the bridge is composed of two fluid resistances: one orifice-type resistance and one capillary-type resistance.

The pressure drop, δP_N, across an orifice is a nonlinear function of the volumetric flow, Q, given by the following:[1]

$$\delta P_N = K Q^2 \tag{A-1}$$

The loss coefficient of a circular orifice, K, is a function of the orifice diameter, d, the density, ρ, and the discharge coefficient, C_d.

$$K = b \rho \tag{A-2}$$

Where the geometric term is defined as follows.

$$b = \frac{8}{\pi^2 d^4 C_d^2} \tag{A-3}$$

The discharge coefficient, C_d, is dependent upon the operating pressure drop. Generally, C_d is constant for turbulent operation; whereas, C_d is quite variable for laminar operation. As a general guideline, the flow through an orifice is turbulent if the Reynolds number, N_r, is in excess of 1000.

$$N_r = \frac{4Q \rho}{\pi d \mu} = d\, C_d \sqrt{\frac{2\, \delta P_N}{\mu^2/\rho}} \geq 1000. \tag{A-4}$$

Thus, the pressure drop across the orifice should be greater than the following:

$$\delta P_N \geq 5.0 \times 10^5 \; \frac{\mu^2}{\rho} \; \frac{1}{d^2 C_d^2} \tag{A-5}$$

The pressure drop, δP_L, across the capillary resistor is a linear function of the volumetric flow rate, Q.

$$\delta P_L = R Q \tag{A-6}$$

---

[1] See the nomenclature for a discussion of the pressure notation.

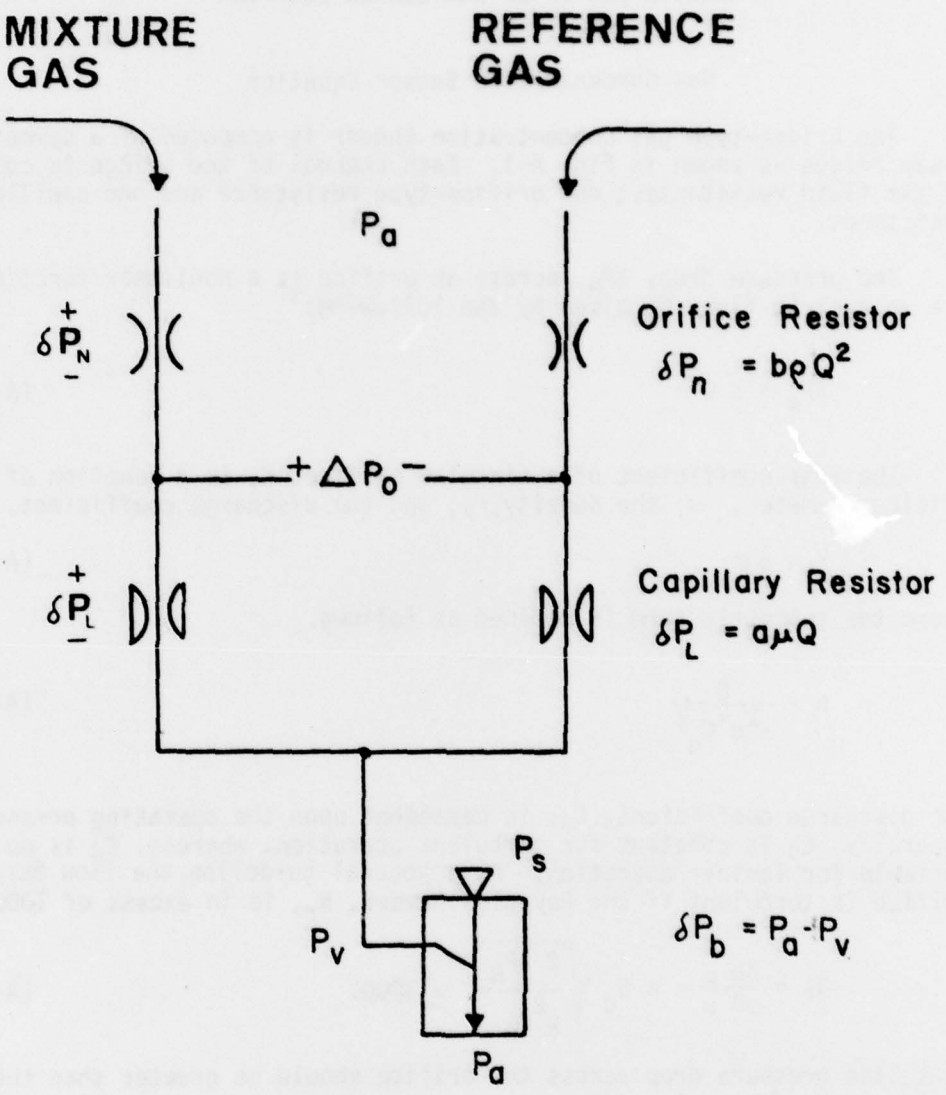

Figure A-1. Bridge-type gas concentration sensor schematic.

The resistive coefficient, R, of a capillary is a function of the length, L, the equivalent hydraulic diameter[2], d_e, the area, A, and the dynamic viscosity, μ.

$$R = a\,\mu \tag{A-7}$$

where

$$a = \frac{32\,L}{A\,d_e^{\,2}} \tag{A-8}$$

For rectangular slots of width, w, and height, h, the geometric term, a, simplifies to the following if $h << w$.

$$a = \frac{10\,L}{w\,h^3} \tag{A-9}$$

The capillary resistance equation above is valid only for laminar flow in which the Reynolds number, N_r, is less than the following:

$$N_r = \frac{Q}{A}\,\frac{d_e}{\mu}\,\rho\,\left(\frac{L}{d_e}\right) = \frac{d_e^{\,2}}{32}\,\frac{\rho}{\mu^2}\,\delta P_L \leq 5.0\times10^4 \tag{A-10}$$

Thus, the pressure drop across the capillary should be less than the following (assuming h/w is small).

$$\delta P_L \leq 5.0\times10^5\,\frac{\mu^2}{\rho}\,\frac{1}{h^2} \tag{A-11}$$

Since the sensor gases are entrained from ambient pressure, P_a, by a vacuum source, P_v, the pressure drop across the sensor bridge[a] is given by that difference, which also is equal to the sum of the drops across the orifice and capillary resistors.

$$\delta P_b = P_a - P_v = \delta P_N + \delta P_L \tag{A-12}$$

The pressure intermediate to the orifice and capillary resistors, P_o, is given as follows:

$$P_o = P_v + \delta P_L \tag{A-13}$$

The pressure drop across the capillary resistor can be expressed as a function of δP_b by solving equations A-1, A-6, and A-12.

$$\frac{\delta P_L}{\delta P_b} = \frac{\sqrt{1 + 4\theta} - 1}{2\theta} \tag{A-14}$$

---

[2]Hydraulic diameter equals four times the area divided by the perimeter of the cross section.

Where the sensor constant, θ, is defined as

$$\theta = \frac{K}{R^2}\ \delta P_b = \frac{b\,\rho}{a^2\mu^2}\ \delta P_b = \frac{\delta P_N}{\delta P_L^2}\ \delta P_b \tag{A-15}$$

The bridge differential output signal is the difference in the two intermediate pressure signals.

$$\Delta P_o = P_{o_{mix}} - P_{o_{ref}} = \delta P_{L_{mix}} - \delta P_{L_{ref}} \tag{A-16}$$

By using equation A-14:

$$\frac{\Delta P_o}{\delta P_b} = \left[\frac{\sqrt{1 + 4\zeta\theta_r} - 1}{2\zeta\theta_r}\right] - \left[\frac{\sqrt{1 + 4\theta_r} - 1}{2\theta_r}\right] \tag{A-17}$$

Where θ_r is the sensor constant evaluated with the reference gas, and the principal sensor variable, ζ, is the ratio of the sensor constants in the mixture and reference channels.

$$\zeta = \frac{\theta_m}{\theta_r} = \frac{b_m/b_r}{(a_m/a_r)^2}\ \frac{\rho_m/\rho_r}{(\mu_m/\mu_r)^2} \tag{A-18}$$

As can be seen, ζ can be considered as a function of two independent variables, the geometric symmetry constant, σ, and the gas properties variable, γ, defined as follows:

$$\sigma = \frac{b_m/b_r}{(a_m/a_r)^2} \tag{A-19}$$

$$\gamma = \frac{\rho_m/\rho_r}{(\mu_m/\mu_r)^2} \tag{A-20}$$

Notice that $\sigma = 1.0$ for a symmetrical bridge and that γ varies with the concentration of the mixture.

Hence the output equation becomes

$$\frac{\Delta P_o}{\delta P_b} = \left[\frac{\sqrt{1 + 4\sigma\gamma\theta_r} - 1}{2\sigma\gamma\theta_r}\right] - \left[\frac{\sqrt{1 + 4\theta_r} - 1}{2\theta_r}\right] \tag{A-21}$$

in which γ is a function of the gas concentration.

Equation A-21 is quite nonlinear looking and the relation for γ as a function of concentration also is nonlinear as given in Appendix B. Thus, the output equation is linearized with respect to the sample gas concentration X_S, about the point $X_S = 0$ and $\sigma = 1.0$ (thus $\gamma = 1.0$).

$$\frac{\Delta P_o}{\delta P_b}(X_s) = \frac{\Delta P_o}{\delta P_b}\bigg|_{\gamma=1.0} + \frac{\partial \Delta P_o/\delta P_b}{\partial \gamma}\frac{\partial \gamma}{\partial X_s}\bigg|_{\gamma=1.0} X_s + \frac{\partial \Delta P_o/\delta P_b}{\partial \sigma}\bigg|_{\sigma=1.0} (\sigma-1) \qquad \text{(A-22)}$$

At $X_s = 0$ and $\sigma = 1.0$, $\Delta P_o/\delta P_b$ is zero which makes the first term vanish.

$$\frac{\Delta P_o}{\delta P_b} = G_b\, S_b\, X_s + G_b\,(\sigma-1) = G_b\, S_b\,(X_s - X_{so}) \qquad \text{(A-23)}$$

Where X_{so} is an equivalent concentration to produce an output without any sample gas present.

The sensor gain function, G_b, is a function of the sensor constant, θ, evaluated with the reference gas.

$$G_b = \frac{\partial \Delta P_o/\partial P_b}{\partial \gamma}\bigg|_{\gamma=1.0} = \frac{\partial \Delta P_o/\delta P_b}{\partial \sigma}\bigg|_{\sigma=1} = \frac{\sqrt{1+4\theta} - 2\theta - 1}{2\theta\sqrt{1+4\theta}} \qquad \text{(A-24)}$$

The gas sensitivity coefficient, S_b, is a function only of the sample and reference gases and is derived in Appendix B and tabulated for several gases.

$$S_b = \frac{\partial \gamma}{\partial X_s}\bigg|_{X_s = 0} \qquad \text{(A-25)}$$

The asymmetry of the bridge gives rise to a constant term in equation A-23 which is the same offsetting effect as having a constant added concentration. Considering only a symmetrical bridge yields the final linearized equation for the bridge gas concentration sensor

$$\frac{\Delta P_o}{\delta P_b} = G_b\, S_b\, X_s \qquad \text{(A-26)}$$

The gain function, G_b, affects the apparent gain of the sensor since S_b is a constant for given gases. G_b varies with the sensor constant and has an absolute maximum of -0.1716 at $\theta = 1.207$ as shown by Figure A-2.

The validity and accuracy of all linearizations are given in reference 6 and are not repeated here except to say that all linearizations are within engineering tolerances for the gases of interest.

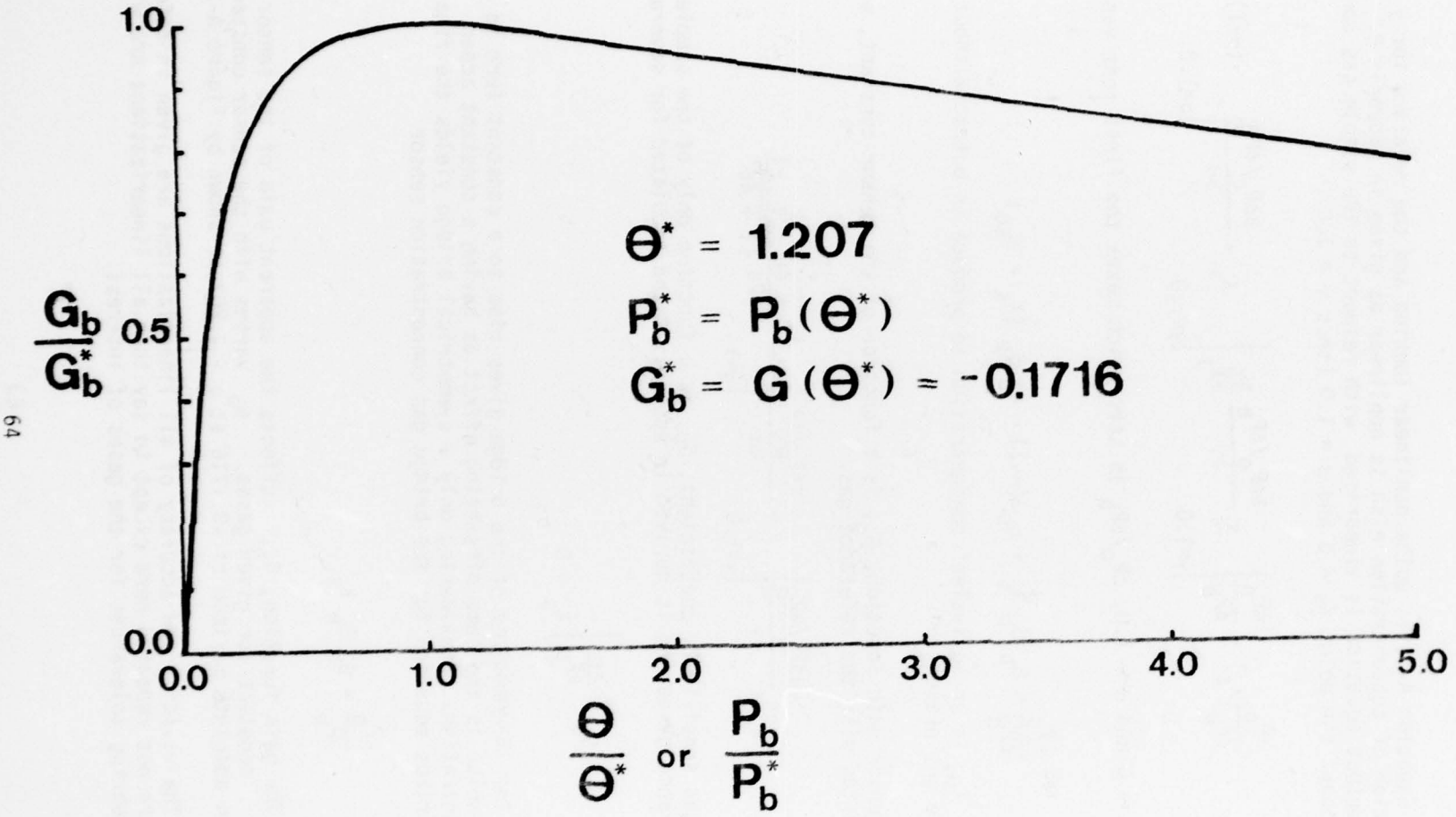

Figure A-2. The sensor gain function.

Partial Pressure Sensor Equation

The volumetric concentration of one gas in a mixture, X_s, is also equal to the ratio of the partial pressure of that gas, P_{as}, to the total pressure, P_a. Thus, the partial pressure can be expressed as the product of concentration and total pressure.

$$P_{as} = X_s P_a \tag{A-27}$$

The gas concentration sensor accurately senses X_s and can be made to sense partial pressure if the bridge pressure drop is made to vary in proportion to P_a as can be seen by rearrangement of the concentration sensor equation derived in the previous section.

$$\Delta P_o = G_b S_b X_s \delta P_b \tag{A-28}$$

The gain function, G_b, is a relatively constant function; S_b is a constant, and δP_b can be made to vary in proportion to P_a by use of the compressible characteristics of the ejector. Once the ejector becomes choked, further decreases in downstream pressure have no effect upon the vacuum produced as shown by Figure 7.

Considering the loading effects on the ejector, the ejector performance when driving the bridge can be modeled by the following.

$$\delta P_b = P_a - P_v = C_1(P_a - P_{ao}) \tag{A-29}$$

In the above, C_1 is the slope and P_{ao} is the intercept.

The output equation reduces to the following:

$$\Delta P_o = G_b S_b C_1 X_s (P_a - P_{ao}) \tag{A-30}$$

Since $G_b S_b C_1$ is relatively constant, and $X_s P_a$ is partial pressure, the sensor effectively senses partial pressure of the sample gas if P_{ao} is small.

$$\Delta P_o = G_T P_{as} \tag{A-31}$$

Where the total gain, G_T, is given by:

$$G_T = G_b S_b C_1 \tag{A-32}$$

In the partial pressure sensing application, special attention must be paid to the sensor constant and corresponding gain function since both ρ and δP_b are changing. From the previous section, θ is given by the following when ρ and δP_b vary (ρ_{SL} and P_{SL} are the density and pressure at sea level).

$$\theta = \frac{b/a^2}{\mu^2/\rho_{SL}} C_1 \frac{P_a}{P_{SL}}(P_a - P_{ao}) \tag{A-33}$$

Assuming P_{ao} to be small, it can be seen that θ varies with the square of P_a and hence G_b changes significantly with P_a. This effect is somewhat overcome by selecting θ much larger than the optimum at sea level. As P_a decreases (increasing altitude) θ decreases and hence the gain slowly increases to the maximum gain and then decreases rapidly as can be seen in Figure A-2.

APPENDIX B

COMPUTATION OF GAS MIXTURE PROPERTIES

The gas concentration sensor is sensitive to the gas properties variable, γ.

$$\gamma = \frac{\rho_m/\rho_r}{(\mu_m/\mu_r)^2} \tag{B-1}$$

The density and viscosity of the mixture gas vary according to the volumetric concentrations (or mole fractions) of the sample gases mixed with the reference gas.

The density of a mixture, ρ_m, is a linear function of the densities and the mole fractions of the constituents present (n = number of different gases; i = 1 implies reference gas, 2 = first sample gas, etc.)

$$\rho_m = \sum_{i=1}^{n} X_i \rho_i \tag{B-2}$$

For any mixture, the mole fractions always sum to unity.

$$\sum_{i=1}^{n} X_i = 1.0 \tag{B-3}$$

The density of a binary mixture (one sample gas, s, in the reference gas, r) can be expressed from B-2 and B-3 as follows.

$$\frac{\rho_m}{\rho_r} = 1 + X_s \left(\frac{\rho_s}{\rho_r} - 1\right) \tag{B-4}$$

The gas viscosity, however, cannot be calculated by such a simple equation due to gas diffusion. As shown by Wilke [16] the gas viscosity of a mixture, μ_m, can be accurately estimated by the following:

$$\mu_m = \sum_{i=1}^{n} \frac{\mu_i}{\left(1 + \frac{1}{X_i} \sum_{\substack{j=1 \\ j\neq i}}^{n} X_j \phi_{ij}\right)} \tag{B-5}$$

Where the constant ϕ_{ij} is given by the following equation and is tabulated in Table B-1 for common gases.

$$\phi_{ij} = \frac{1}{\sqrt{8\left(1 + \frac{\rho_i}{\rho_j}\right)}} \left[1 + \sqrt[4]{\frac{(\mu_i/\mu_j)^2}{(\rho_i/\rho_j)}}\right]^2 \qquad (B\text{-}6)$$

The viscosity of a binary mixture with a sample concentration, X_s, reduces to the following.

$$\frac{\mu_m}{\mu_r} = \frac{1}{1 + \frac{X_s}{1-X_s}\phi_{rs}} + \frac{\mu_s/\mu_r}{1 + \frac{1-X_s}{X_s}\phi_{sr}} \qquad (B\text{-}7)$$

The gas properties variable, γ, for a binary mixture can be calculated from equations B-1, B-4, and B-7. This results in an equation that is nonlinear in X_s. However, for the linearized analysis presented in Appendix A, only the partial derivative is required to determine the gas sensitivity constant, S_b. It can be shown that S_b reduces to the following expression.

$$S_b = \left.\frac{\partial \gamma}{\partial X_s}\right|_{X_s=0} = \left(\frac{\rho_s}{\rho_r} - 1\right) - 2\left\{\frac{\mu_s/\mu_r}{\phi_{sr}} - \phi_{rs}\right\} \qquad (B\text{-}8)$$

The gas sensitivity constant, S_b, is a function only of the sample and reference gas properties and is tabulated for various gases in Table B-2.

TABLE B-1. ϕ FOR GAS VISCOSITY CALCULATIONS

i	j	ρ_i/ρ_j	μ_i/μ_j	ϕ_{ij}
O_2	Air	1.1053	1.1038	0.99875
Air	O_2	0.9047	0.9060	1.00029
CO_2	Air	1.5291	0.8081	0.72700
Air	CO_2	0.6540	1.2375	1.37583
H_2O	Air	0.6216	0.4918	0.88939
Air	H_2O	1.6088	2.0333	1.12409
O_2	CO_2	0.7228	1.3659	1.38497
CO_2	O_2	1.3835	0.7321	0.73289
H_2O	CO_2	0.4065	0.6086	1.16521
CO_2	H_2O	2.4599	1.6431	0.77830
H_2O	O_2	0.5624	0.4456	0.88698
O_2	H_2O	1.7782	2.2444	1.11950

TABLE B-2. GAS SENSITIVITY CONSTANT, S_b

Sample	Reference	ρ_s/ρ_r	μ_s/μ_r	S_b
CO_2	Air	1.5291	0.8081	1.0555
O_2	Air	1.1053	1.1038	-0.1045
H_2O	Air	0.6216	0.4918	0.7639
CO	Air	0.9671	0.9563	0.0549
N_2	Air	0.9673	0.9563	0.0551
CH_4	Air	0.5544	0.5940	0.2828
C_2H_6	Air	1.0493	0.4923	1.6773
C_3H_8	Air	1.5544	0.4372	2.9827
C_4H_{10}	Air	2.0856	0.3989	4.2807
C_5H_{12}	Air	2.6150	0.3634	5.6311
C_8H_{18}	Air	4.1508	0.2896	9.6577
CO_2	N_2	1.5808	0.8457	0.9867
O_2	N_2	1.1427	1.1543	-0.1675
N_2	O_2	0.8751	0.8663	0.1410
Air	O_2	0.9047	0.9060	0.0818
H_2O	O_2	0.5623	0.4455	0.7967

APPENDIX C

THE STANDARD ATMOSPHERE AND CONVERSIONS*

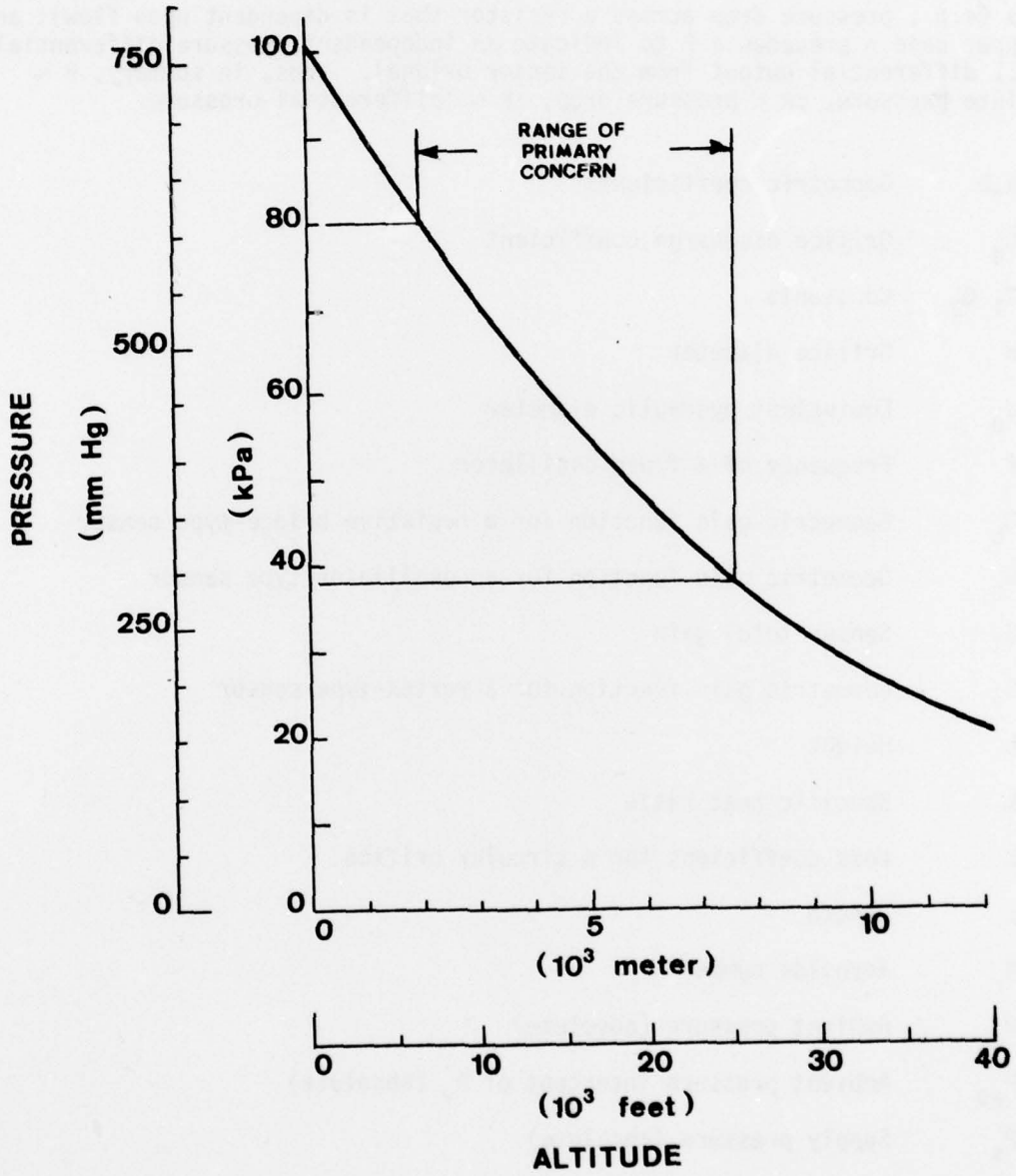

* The U.S. Standard Atmosphere (45° north latitude, July), U.S. Government Printing Office, 1966.

LIST OF ABBREVIATIONS AND SYMBOLS

NOTE: *The following notation will be strictly used in this report to distinguish between absolute pressure, pressure drop, and differential pressure:* A capital P with no prescript is used to indicate pressure measured in an absolute sense; a lower case δ precedes a P to indicate dependent-type pressure drops (e.g., pressure drop across a resistor that is dependent upon flow); and an upper case Δ precedes a P to indicate an independent pressure differential (e.g., differential output from the sensor bridge). Thus, in summary, P $\sim$ absolute pressure, $\delta P \sim$ pressure drop, $\Delta P \sim$ differential pressure.

a,b	Geometric coefficients
C_d	Orifice discharge coefficient
C_1 C_2	Constants
d	Orifice diameter
d_e	Equivalent hydraulic diameter
f	Frequency of a fluid oscillator
G_b	Geometric gain function for a resistive bridge-type sensor
G_o	Geometric gain function for an oscillator-type sensor
G_T	Sensor total gain
G_v	Geometric gain function for a vortex-type sensor
h	Height
k	Specific heat ratio
K	Loss coefficient for a circular orifice
L	Length
N_r	Reynolds number
P_a	Ambient pressure (absolute)
P_{ao}	Ambient pressure intercept of P_v (absolute)
P_s	Supply pressure (absolute)
P_v	Pressure at vacuum port of ejector (absolute)
$P_{\partial s}$	Partial pressure of sample gas

Q	Gas flow rate (volumetric basis)
R_r	Gas constant
R	Resistive coefficient for a capillary resistor
R_o	Ejector output resistance
S_b	Gas sensitivity constant for a bridge-type sensor
S_o	Gas sensitivity constant for an oscillator-type sensor
S_v	Gas sensitivity constant for a vortex-type sensor
T_a	Ambient temperature (absolute)
w	Width
X	Concentration ratio (or mole fraction)
γ	Gas properties variable
Δf	Beat frequency
ΔP_o	Differential output pressure signal
δP_b	Pressure drop across a gas concentration sensor
δP_L	Pressure drop across a capillary resistor
δP_N	Pressure drop across an orifice
ζ	Principal sensor variable
θ	Sensor constant for a bridge-type sensor
μ	Dynamic viscosity
ρ	Density
σ	Geometric symmetry constant
ϕ_{rs}, ϕ_{sr}	Constants approximately equal to unity

SUBSCRIPTS:

m	Mixture
r	Reference
s	Sample